Uncertainty and Business Cycles: New Insights Post-COVID-19

a contribution to Angelini G., Bacchiocchi E., Caggiano G. and Fanelli L. (2018) "Uncertainty Across Volatility Regimes"

Pondini Riccardo

1 Introduction

In this paper, we analyze a topic that has garnered interest since the global financial crisis: whether the uncertainty in macroeconomic and financial variables can be considered a driver of the business cycle. In the paper *"Uncertainty Across Volatility Regimes"* by Angelini G., Bacchiocchi E., Caggiano G., and Fanelli L. (2018), this topic was explored. However, given the limited data available at that time, their analysis concluded before the onset of the COVID-19 pandemic. This period has had a significant impact on economic and financial dynamics, as well as on the behavior of households and firms. Given these developments, it is crucial to study this subject with the additional insights provided by these challenging times.

The main findings of this paper, in line with the previous work, are as follows: First, heightened uncertainty leads to an overall contraction in real economic activity. Second, uncertainty tends to increase during economic recessions (see Figure 1). Third, the effects of uncertainty shocks vary over time. The first finding aligns with the views of Christiano, Motto, & Rostagno (2014), who demonstrated how incorporating entrepreneurs and financial frictions into a Dynamic Stochastic General Equilibrium (DSGE) model clarifies the impact of risk shocks on the economy. Increased uncertainty results in higher credit spreads, which in turn reduces the availability of credit for entrepreneurs. This decrease in credit availability leads to lower investment and subsequent declines in output, consumption, and employment. These findings illustrate that uncertainty shocks produce countercyclical credit spreads and contractionary effects on major economic indicators, closely reflecting observed patterns in U.S. business cycles.

However, an exception occurs during the fourth volatility regime (a concept to be elucidated in the next part of the section), where, despite rising measures of uncertainty, economic activity appears to increase due to extreme measures taken by the Federal Reserve and subsidies provided by the U.S. government after the 2020. The real negative impact of these unexpected positive uncertainty shocks appears to manifest with a delay, while their immediate impact is positive (see Section 3.5 for Impulse response functions). During the initial phase of the COVID-19 impact, uncertainty increased significantly alongside a sharp decline in economic activity. As the pandemic progressed, downside risks greatly diminished. By early 2021, while the forecast distribution remained highly dispersed, indicating that subjective uncertainty was still elevated, it increasingly reflected upside rather than downside risks (see also *COVID-19 Uncertainty: A Tale of Two Tails*, 2021). This observation aligns also with the growth options theory and highlights potential differences in dynamics across sectors [1], which will be discussed in detail in Sections 3.3 and 3.5. These expansionary effects of uncertainty are not new in the literature. Segal et al. (2015), for example, challenge the prevailing view that uncertainty invariably exerts a negative effect on economic activities. They propose a novel perspective suggesting that uncertainty might be beneficial for business activities, particularly when considering future industrial prospects. They cite the high-tech revolution of the 1990s as an example, noting the difficulty in predicting specific outcomes while recognizing the widespread belief among analysts and specialists that many firms would benefit from emerging technologies.

The authors develop a theoretical model accommodating both negative and positive uncertainty shocks. This dual effect allows uncertainty to exert opposing impacts. Empirically, they confirm the existence of a positive uncertainty component using a Vector Autoregression (VAR) model. Furthermore, they utilize the predictable component of this measure to capture ex-ante uncertainty, demonstrating that positive uncertainty shocks have lasting beneficial effects on several key macroeconomic variables and mitigate the adverse impacts of negative shocks.

The second finding regarding the countercyclicality of uncertainty aligns with the concept of "endogenous uncertainty," which suggests that uncertainty is more often a consequence of the business cycle than its cause. However, it also supports the contrary perspective that recessions may be triggered by exogenous increases in uncertainty measures. Specifically, in this paper, uncertainty appears to be an exogenous driver with respect to economic activity, as the immediate effect of economic activity on uncertainty is not significantly different from zero. Nonetheless, our model does not rule out the possibility of delayed endogenous effects of real economic activity on uncertainties.

The variability in the relationship between uncertainty and real economic activity over time aligns with theoretical models which emphasize that the impacts of increased uncertainty are more pronounced under extreme conditions, such

[1] It must be acknowledged, however, that there is no single theory of uncertainty or comprehensive structural model that directly translates to empirical data application. Essentially, while the existing theoretical work facilitates the justification and prediction of relationships, it fails to provide precise identifying restrictions for empirical analysis. Instead, the literature offers a broad spectrum of theoretical predictions regarding the relationship between uncertainty and real economic activity. These predictions must be theoretically consolidated and then empirically validated through data.

as significant financial crises. This view is supported by the findings of Alfaro, I. N., Bloom, N., & Lin, X. (2018) and Chiara Scotti (2023), who demonstrated that the effects on GDP are significantly stronger when analyzing impulse response functions to negative macroeconomic and financial shocks during periods of high volatility compared to low volatility. Additionally, our analysis reveals that the transmission of financial uncertainty to real economic activity is predominantly indirect: financial uncertainty shocks lead to macroeconomic uncertainty, which then triggers a contraction in real activity. This impact varies by economic regime, resulting in a direct and marked effect of ε_{Ft} during periods of intense financial stress, such as the COVID-19 + Recovery period, further demonstrating the variability of the relationship between uncertainty and economic activity.

The question of whether causality flows from uncertainty to real economic activity, from real activity to uncertainty, or operates bidirectionally, as well as how this relationship may vary under different macroeconomic conditions, can be empirically examined using a structural vector autoregression (SVAR) framework. Addressing this issue requires moving beyond recursive identification schemes, which are inherently limited in their ability to analyze reverse causality. Additionally, it necessitates moving beyond linear SVARs, which cannot capture potentially regime-dependent effects of uncertainty shocks.

To address these limitations, this paper employs a non-recursively identified SVAR model that leverages information derived from breaks in the unconditional volatility of the macroeconomic variables under consideration. Although recursive schemes are still quite popular among VAR macroeconomists, more often than not, the non-recursive schemes implied by DSGE models are unfeasible due to insufficient information obtained from the reduced-form variance–covariance matrix. This novel approach instead, enables us to test identification schemes -provided a necessary and sufficient rank condition is respected- that account for the endogeneity and reverse causality previously discussed, as well as the regime dependence of these effects. This approach is defined "identification through heteroskedasticity" and has been already adopted by Rigobon (2003), and Lanne and Lütkepohl (2008). Similarly to these authors, we exploit the presence of breaks in the VAR covariance matrix to identify the structural shocks of interest. Differently from these authors, however, we remove the assumption that structural breaks affect only the error covariance matrix and leave the impulse vectors unchanged. In our framework, a variation in the VAR covariance matrix can be linked to changes in the structural parameters; thus, our analysis for identifying the real impacts of uncertainty shocks employs a more comprehensive approach that also accounts for varying dynamics across different regimes (see Section 2.4 for the comparison of the two approaches).

We estimate a small scale SVAR with three variables, a measure of economic activity Y_t, a measure of macroeconomic uncertainty U_{Mt} and a measure for financial uncertainty U_{Ft}. Real activity is proxied by industrial production or employment and the two index of uncertainties are taken from Sydney C. Ludvigson database. The data are monthly and span the 1960:M8–2024:M6 sample. Using recursive and rolling-window estimates of the VAR covariance matrix, we identify three major volatility breaks that align with significant episodes in U.S. economic history: the onset of the Great Moderation, the Global Financial Crisis (GFC) of 2007–2008, and the COVID-19 pandemic. These breaks define four distinct macroeconomic regimes: the "Great Inflation" period (1960:M8–1984:M3), the "Great Moderation" period (1984:M4–2007:M12), the "Great Recession + Slow Recovery" period (2008:M1–2019:M11), and the "COVID-19 + Recovery" period (2019:M12–2024:M6).

The "COVID-19 + Recovery" regime reflects the unique dynamics of the pandemic, characterized by unprecedented policy measures, heightened uncertainty, and an initially sharp contraction in economic activity followed by a rapid but uneven recovery. The inclusion of this additional regime allows us to capture the distinct identification information associated with this period.

To analyze these regimes, we identify shocks by specifying a non-recursive structural model that leverages differences in the average level of volatility observed across these four subsamples.

Overall, our findings support the claim that both macroeconomic and financial uncertainty are exogenous drivers of the business cycle, with contractionary medium-long term effects on real economic activity that vary over time. Consistent with Angelini et al. (2018), macroeconomic uncertainty shocks lead to a decline in U.S. economic activity, with the magnitude of these effects being more pronounced during periods of crisis. Notably, we find that, despite an initial positive effect during the COVID-19 + Recovery regime, the negative impact at a two to three periods horizon is the largest observed across the subsamples (Table 3). This result remains robust when considering alternative measures of real economic activity.

While our findings align with several previous researches in supporting the exogeneity of financial uncertainty, a key contribution of our study is the evidence for the exogeneity of macroeconomic uncertainty. This assumption is rigorously tested within our structural model, and the results do not provide grounds to reject it. To achieve this, we consider three overidentified non-recursive SVAR models (Table 2). One features "endogenous" macroeconomic uncertainty and reverse causality from macroeconomic to financial uncertainty, as proposed by Angelini, Bacchiocchi, Caggiano, and Fanelli (2018). Another incorporates the same characteristics but applies them starting from the third volatility regime onwards. The final model assumes "exogenous" (just on impact) uncertainties, where macroeconomic uncertainty is exogenous with respect to real activity shocks, and financial uncertainty is treated as exogenous in respect to all the other macroeconomic variables shocks. The first two specifications are at the positive edge of the 5% significance level. The additional information provided by the fourth regime slightly improves the first specification compared to Angelini et al. (2018). In contrast, the SVAR featuring "exogenous" macroeconomic uncertainty (along with "exogenous" financial uncertainty) is strongly supported by the data.

Two papers that have previously studied this subject are Ludvigson et al. (2018a) and Carriero et al. (2018b). Both studies address the issue of the exogeneity/endogeneity of uncertainty. Consistent with Ludvigson et al. (2018a), our results support the view that financial uncertainty is exogenous to the business cycle. However, in contrast to their findings and in line with Carriero et al. (2018b), we provide strong evidence that macroeconomic uncertainty is an exogenous driver of the business cycle.

Carriero et al. (2018b) jointly identified real activity and uncertainty shocks by using a novel stochastic volatility approach in the context of VARs that featured measures of macroeconomic and financial uncertainty (one at a time), along with measures of real economic activity. Accordingly, they did not separately identify the effects of macroeconomic and financial sources of uncertainty on economic fluctuations. In fact, as argued in Ludvigson et al. (2018a) and implemented in our paper, the joint use of macroeconomic and financial uncertainty indices is crucial to correctly uncover the relationship between uncertainty and real activity, since these indices can display substantially different properties.

Ludvigson et al. (2018a) introduce a novel identification strategy in a time-invariant framework for simultaneously identifying uncertainty and real activity shocks without imposing restrictions on their contemporaneous relationships. This strategy incorporates two types of shock-based restrictions: event constraints and correlation constraints. Event constraints necessitate that financial uncertainty shocks be significant during major financial disruptions, such as the 1987 stock market crash and the 2007–09 financial crisis. Correlation constraints involve the use of external instruments to introduce additional constraints, thereby refining the identification of the shocks.

In our analysis, similar to Ludvigson et al. (2018a), we observe that the on impact effect of macroeconomic uncertainty on real activity is positive and significant, only during the fourth regime. Additionally, our findings diverge from Ludvigson et al. (2018a), as we also identify a positive contribution from financial uncertainty to this immediate effect during the same period. The paper is organized as follows. Section 2 introduces the identification problem and presents our nonrecursive identification approach. Section 3 discusses the data and the empirical results obtained from the estimated SVAR. Section 4 provides some concluding remarks.

2 Econometric Framework

In this section, we outline our econometric methodology for addressing both regime dependence and the joint identification of uncertainty and real activity shocks. Section 2.1 introduces the general framework and highlights the challenges encountered in "standard" SVARs. Section 2.2 expands the analysis by incorporating the "identification-through-heteroskedasticity" method, a specific case of the more comprehensive approach detailed in Section 2.3. Lastly, Section 2.4 demonstrates how the second method serves as a generalization of the first.

2.1 Standard SVARs, Identifying structural shocks under homoskedasticity

Consider the following SVAR model:

$$X_t = c + \Phi_1 X_{t-1} + \cdots + \Phi_p X_{t-p} + u_t, \quad t = 1, \ldots, T, \tag{1}$$

where X_t is the $n \times 1$ vector of endogenous variables, c is a constant, $\Phi_1, \ldots, \Phi_p$ are $n \times n$ coefficient matrices. The residuals, u_t, are the VAR innovations with variance-covariance matrix different from a diagonal matrix. It is assumed that the autoregressive polynomial $\Phi(L) = I_n - \Phi_1 L - \cdots - \Phi_p L^p$ has roots satisfying $|z| > 1$, ensuring stationarity.

We compact the VAR system in equation (1) into the expression:

$$X_t = \Pi W_t + u_t, \tag{2}$$

where $W_t := (X'_{t-1}, \ldots, X'_{t-p}, 1')'$ and $\Pi := (\phi_1, \ldots, \phi_p, c)$. The VAR reduced form parameters are collected in the p-dimensional vector $\theta := (\pi', \sigma')'$, where $\pi := \text{vec}(\Pi)$ and $\sigma := \text{vech}(\Sigma)$.

The SVAR we consider here is defined by:

$$u_t = B\varepsilon_t, \quad E(\varepsilon_t \varepsilon'_t) := I_n, \quad \Sigma_u = BB', \quad \varepsilon_t \sim WN(0, I_n), \tag{3}$$

where B is a non-singular $n \times n$ matrix of structural parameters and ε_t is an n-dimensional i.i.d. vector of structural shocks with covariance matrix normalized to I_n. As is well known, the system in equations (2)–(3) is unidentified without further restrictions on the elements of the B matrix.

The standard approach for achieving identification involves imposing a set of linear restrictions on B, which can be expressed in an explicit form:

$$\text{vec}(B) := G_B \gamma + g_B, \tag{4}$$

where G_B is an $n^2 \times a_B$ selection matrix, γ is $a_B \times 1$ and contains the 'free' elements of B, and g_B is an $n^2 \times 1$ known vector. The information required to specify the matrix G_B and the vector g_B typically comes from economic theory or from structural and institutional knowledge relevant to the problem being studied.

The condition $a_B = \dim(\gamma) \leq n(n+1)/2$ is necessary for identification. A necessary and sufficient condition for identification is that the $n(n+1)/2 \times a_B$ Jacobian matrix:

$$2D_n^+ (B \otimes I_n) G_B, \tag{5}$$

has full column rank when evaluated in a neighborhood of γ_0, where B_0 represents the counterpart of B that satisfies the restriction $\text{vec}(B_0) := G_B\gamma_0 + g_B$, and γ_0 is the 'true' value of γ.

To avoid confusion, throughout this paper, we refer to the elements in the vector θ as 'reduced form parameters,' while the elements in the vector γ are referred to as 'structural parameters'. If the rank condition in equation (5) holds, the orthogonalized impulse response functions (IRFs) are uniquely identified.

Let A denote the companion matrix of the VAR, such that $X_t^c = (X_t', X_{t-1}', \ldots, X_{t-p+1}')'$ represents the state vector associated with the companion form. Let R be a selection matrix such that $X_t = RX_t^c$. The impulse response function (IRF), which measures the dynamic effect of a structural shock e_{jt} on a variable X_{jt}, is given by:

$$\text{IRF}_j(h) = RA^hR'b_j, \quad h = 0, 1, 2, \ldots, \tag{6}$$

where b_j is the j-th column of B. The IRF at horizon $h = 0$ captures the immediate (on-impact) response of a structural shock, while for $h > 0$, it represents the dynamic response over time.

For this specific study, we assume $n = 3$. Let Y_t denote a scalar measure of real economic activity, and U_{Mt} and U_{Ft} represent scalar measures of macroeconomic and financial uncertainty, respectively. In the absence of additional identifying restrictions, the system is structured as:

$$\begin{pmatrix} u_{Mt} \\ u_{Yt} \\ u_{Ft} \end{pmatrix} = \begin{pmatrix} b_{MM} & b_{MY} & b_{MF} \\ b_{YM} & b_{YY} & b_{YF} \\ b_{FM} & b_{FY} & b_{FF} \end{pmatrix} \begin{pmatrix} \varepsilon_{Mt} \\ \varepsilon_{Yt} \\ \varepsilon_{Ft} \end{pmatrix},$$

The covariance matrix $\Sigma_\eta = BB'$ provides $\frac{n(n+1)}{2} = 6$ symmetry restrictions to identify the 9 elements of B, leaving 3 elements unidentified. If one imposes an upper or lower triangular structure on B, or uses "conventional" zero restrictions, it becomes impossible to simultaneously identify the parameters of interest b_{YM}, b_{YF}, b_{MY}, and b_{FM}. This limitation means that the issues of "endogeneity" and "reverse causality" cannot be adequately addressed.

2.2 Identification through heteroscedasticity

A contribution from Rigobon (2003), and Lanne and Lütkepohl (2008), is a method that exploits the presence of different values that Σ_u may take across subsamples. This variability is a piece of information that can be used in order to identify the structural parameters in study.

Without any loss of generality, we consider a bivariate SVAR model for the vector $X_t = (X_{1,t}, X_{2,t})'$ and assume that the data-generating process belongs to the class of models described by the system (2)–(3). We further assume that at time $t = T_B$, where $1 < T_B < T$, the variance in the data changes such that the two sets of observations $X_1, \ldots, X_{T_B}$ and $X_{T_B+1}, \ldots, X_T$ are characterized by two distinct VAR covariance matrices $\Sigma_{u,1}$ and $\Sigma_{u,2}$, respectively, where:

$$\Sigma_{u,i} := \begin{pmatrix} \sigma_{11.i} & \sigma_{12.i} \\ \sigma_{21.i} & \sigma_{22.i} \end{pmatrix}, \quad i = 1, 2.$$

Consider the relationship $u_t := B\varepsilon_t$, where ε_t is the vector of structural shocks. Rigobon's (2003) identification approach is based on the joint use of the moment conditions:

$$\Sigma_{u,1} = B\Lambda_1B', \quad \Sigma_{u,2} = B\Lambda_2B', \tag{7}$$

where B, Λ_1, and Λ_2 are defined as:

$$B := \begin{pmatrix} b_{11} & b_{12} \\ b_{21} & b_{22} \end{pmatrix}, \quad \Lambda_1 := \begin{pmatrix} \lambda_{11.1} & 0 \\ 0 & \lambda_{22.1} \end{pmatrix}, \quad \Lambda_2 := \begin{pmatrix} \lambda_{11.2} & 0 \\ 0 & \lambda_{22.2} \end{pmatrix}.$$

The matrices Λ_1 and Λ_2 collect the variances in the structural shocks across the two volatility regimes. Equation (7) links the reduced-form coefficients $\sigma_+ := (\text{vech}(\Sigma_{u,1})', \text{vech}(\Sigma_{u,2})')' = (\sigma_{11.1}, \sigma_{22.1}, \sigma_{21.1}, \sigma_{11.2}, \sigma_{22.2}, \sigma_{21.2})'$ to the structural form parameters in B, Λ_1, and Λ_2. As is standard in the SVAR literature, Λ_1 is normalized to be the identity matrix, I_2. The six structural parameters $\gamma := (b_{11}, b_{12}, b_{21}, b_{22}, \lambda_{11.2}, \lambda_{22.2})'$ can be uniquely recovered from σ_+ by solving system (7).

This identification approach has been extended by Lanne and Lütkepohl (2008) to the case of SVARs, where $\dim(X_t) = n > 2$. The 'purely statistical' approach to the identification of SVARs introduced by Rigobon (2003) and Lanne and Lütkepohl (2008) has significant implications for the transmission mechanisms of shocks. In their framework, the structural break at time T_B affects only the VAR error covariance matrix, and hence the IRFs computed on the subsamples $X_1, \ldots, X_{T_B}$ and $X_{T_B+1}, \ldots, X_T$ remain unchanged, meaning they exhibit the same time patterns across the two volatility regimes.

2.3 Novel approach by Bacchiocchi, E., & Fanelli, L. (2015)

Our paper contributes to the literature of identification through heteroskedasticity by relaxing the restrictive assumption that changes in the volatility of the data have no impact on the transmission mechanisms of the shocks. In particluar the main feature of the method exploited in this paper and presented in Bacchiocchi, E., & Fanelli, L. (2015) but also in Angelini G., Bacchiocchi E., Caggiano G. and Fanelli L. (2018), is that not only Σ_u may take different values across subsamples, but also that the elements in B may change across volatility regimes, generating regime-dependent IRFs. Allowing for changes in the structural parameters B, represents a major generalization relative to the "standard" identification approach based on heteroskedasticity developed in Rigobon (2003), Lanne and Lütkepohl (2008). Another important characteristic of this approach is that it also accounts for cases where the slope (autoregressive) parameters vary across volatility regimes ($\Pi_1 \neq \Pi_2 \neq \Pi_3 \neq \Pi_4$). This variation represents another potential cause of regime dependency in the IRFs. We remark that, even in the special case where the slope (autoregressive) coefficients remain constant across volatility regimes, the IRFs generated by this approach still differ across regimes due to changes in the on-impact response coefficients.

Going back to the SVAR for $X_t := (U_{Mt}, Y_t, U_{Ft})'$ defined in Equation 1, consider the unconditional covariance matrix Σ_u:

$$\Sigma_u = E(u_t u_t') := \begin{pmatrix} \sigma_M^2 & \sigma_{M,Y} & \sigma_{M,F} \\ & \sigma_Y^2 & \sigma_{Y,F} \\ & & \sigma_F^2 \end{pmatrix}, \tag{8}$$

where $\sigma_{M,Y} = E(u_{Mt}u_{Yt})$, $\sigma_{M,F} = E(u_{Mt}u_{Ft})$, and $\sigma_{Y,F} = E(u_{Yt}u_{Ft})$.

Assume that there are three structural changes in this unconditional error covariance matrix, corresponding to the existence of four distinct volatility regimes. If $t = T_{B_1}$, $t = T_{B_2}$ and $t = T_{B_3}$ denote the dates of the three structural breaks, with $1 < T_{B_1} < T_{B_2} < T_{B_3} < T$, the reduced-form VAR in Equation 1 can be generalized to:

$$X_t = \Pi(t)W_t + u_t, \quad \Sigma_u(t) := E(u_t u_t'), \quad t = 1, \ldots, T, \tag{9}$$

where $W_t := (X_{t-1}', \ldots, X_{t-p}', 1)'$ contains lagged regressors and a constant, and $\Pi(t)$ is the matrix of associated slope (autoregressive) coefficients given by:

$$\Pi(t) := \Pi_1 \times 1(t \leq T_{B_1}) + \Pi_2 \times 1(T_{B_1} < t \leq T_{B_2}) + \Pi_3 \times 1(T_{B_2} < t \leq T_{B_3}) + \Pi_4 \times 1(t > T_{B_3}), \tag{10}$$

and, finally, the error covariance matrix $\Sigma_\eta(t)$ is given by:

$$\Sigma_u(t) := \Sigma_{u,1} \times 1(t \leq T_{B_1}) + \Sigma_{u,2} \times 1(T_{B_1} < t \leq T_{B_2}) + \Sigma_{u,3} \times 1(T_{B_2} < t \leq T_{B_3}) + \Sigma_{u,4} \times 1(t > T_{B_3}). \tag{11}$$

Given the existence of four volatility regimes, the SVAR is defined by the structural specification:

$$u_t = \begin{cases} B\varepsilon_t, & t \leq T_{B_1}, \\ (B + Q_2)\varepsilon_t, & T_{B_1} < t \leq T_{B_2}, \\ (B + Q_2 + Q_3)\varepsilon_t, & T_{B_2} < t \leq T_{B_3}, \\ (B + Q_2 + Q_3 + Q_4)\varepsilon_t, & T_{B_3} < t \leq T, \end{cases} \tag{12}$$

where B, Q_2, Q_3 and Q_4 are 3×3 matrices containing structural parameters, and $\varepsilon_t := (\varepsilon_{Mt}, \varepsilon_{Ft}, \varepsilon_{Yt})'$ is the vector of structural shocks. Here, ε_{Mt} denotes the "macroeconomic uncertainty shock," ε_{Ft} the "financial uncertainty shock," and ε_{Yt} the "shock to real activity."[2]

In Equation 12, B is the nonsingular matrix defining the structural contemporaneous relationships (on-impact responses) among variables and shocks for the first volatility regime. The matrix Q_2 captures any changes in structural parameters transitioning from the first to the second volatility regime, while $B + Q_2$ defines these relationships in the second regime. Similarly, Q_3 accounts for changes from the second to the third volatility regime, with $B + Q_2 + Q_3$ describing the structural relationships in the third regime. Lastly, Q_4 captures changes from the third to the fourth volatility regime, with $B + Q_2 + Q_3 + Q_4$ representing the relationships in the fourth regime.

Equation 12 leads to the system of second-order moment conditions:

$$\Sigma_{u,1} = BB', \tag{13}$$
$$\Sigma_{u,2} = (B + Q_2)(B + Q_2)', \tag{14}$$
$$\Sigma_{u,3} = (B + Q_2 + Q_3)(B + Q_2 + Q_3)', \tag{15}$$
$$\Sigma_{u,4} = (B + Q_2 + Q_3 + Q_4)(B + Q_2 + Q_3 + Q_4)'. \tag{16}$$

[2] As highlighted in Ludvigson et al. (2018a) and Angelini G., Bacchiocchi E., Caggiano G., and Fanelli L. (2018), the structural shocks identified in our analysis do not necessarily correspond to the primitive shocks of any specific model, as this is not our primary objective. Our real activity shocks may originate from various sources, such as technological changes, monetary policy innovations, preference shifts, or government expenditure fluctuations. Financial uncertainty shocks could emerge due to expected volatility in financial markets, such as fears of a bank run or concerns over bankruptcy. Similarly, macroeconomic uncertainty shocks could arise from anticipated volatility in the macroeconomy. This could include expectations of greater difficulty in forecasting future productivity, monetary policy, or fiscal policy.

The total number of elements in B, Q_2, Q_3 and Q_4 is $4n^2$; hence, it is necessary to impose at least $4n^2 - \frac{4}{2}n(n+1) = \frac{4}{2}n(n-1) = 12$ additional constraints to achieve identification. The identifying constraints are provided by economic reasoning about the way the on-impact coefficients may change across regimes, which means that the suggested identification approach combines both data properties (i.e., the heteroskedasticity provided by the data) and theoretical considerations.

Let ψ be the vector defined as:

$$\psi := (\text{vec}(B)', \text{vec}(Q_2)', \text{vec}(Q_3)', \text{vec}(Q_4)')'.$$

The set of theory-based linear identifying restrictions on B, Q_2, Q_3 and Q_4 can be represented compactly in explicit form by:

$$\psi = G\gamma + g, \tag{17}$$

where γ is the vector containing the "free" elements in B, Q_2, Q_3 and Q_4, G is a known $4n^2 \times \dim(\gamma)$ selection matrix of full column rank, and $g := (g'_B, g'_{Q_2}, g'_{Q_3}, g'_{Q_4})'$ is a $4n^2 \times 1$ vector containing known elements.

By writing the relation between the reduced form parameters and the structural one as:

$$\sigma_+ = g(\gamma), \tag{18}$$

where $\sigma_+ := (\text{vech}(\Sigma_{u,1})', \text{vech}(\Sigma_{u,2})', \text{vech}(\Sigma_{u,3})', \text{vech}(\Sigma_{u,4})')'$ is an $\frac{4}{2}n(n+1) \times 1$ vector, and $g(\cdot)$ is a nonlinear (differentiable) vector function, it turns out that the necessary and sufficient rank condition for identification is still that the Jacobian matrix:

$$J(\gamma) := \frac{\partial g(\gamma)}{\partial \gamma'}$$

or also

$$\left(I_4 \otimes D_n^+\right) \begin{pmatrix} (B \otimes I_n) & 0_{n^2 \times n^2} & 0_{n^2 \times n^2} & 0_{n^2 \times n^2} \\ (B + Q_2) \otimes I_n & (B + Q_2) \otimes I_n & 0_{n^2 \times n^2} & 0_{n^2 \times n^2} \\ (B + Q_2 + Q_3) \otimes I_n & (B + Q_2 + Q_3) \otimes I_n & (B + Q_2 + Q_3) \otimes I_n & 0_{n^2 \times n^2} \\ (B + Q_2 + Q_3 + Q_4) \otimes I_n & (B + Q_2 + Q_3 + Q_4) \otimes I_n & (B + Q_2 + Q_3 + Q_4) \otimes I_n & (B + Q_2 + Q_3 + Q_4) \otimes I_n \end{pmatrix} G$$

be regular and of full column rank when evaluated in a neighborhood of the true parameter value γ_0 as in the standard case.

We denote $\tilde{B} = B(\theta), \tilde{Q}_2 = Q_2(\theta), \tilde{Q}_3 = Q_3(\theta)$ and $\tilde{Q}_4 = Q_4(\theta)$ as the counterparts of B, Q_2, Q_3 and Q_4 which fulfill the identification conditions. As previously mentioned, the necessary condition for identification requires imposing at least twelve joint restrictions on the matrices of structural parameters.

However, the configurations of $\tilde{B}$ (for the first regime), $(\tilde{B} + \tilde{Q}_2)$ (for the second regime), $(\tilde{B} + \tilde{Q}_2 + \tilde{Q}_3)$ (for the third regime), and $(\tilde{B} + \tilde{Q}_2 + \tilde{Q}_3 + \tilde{Q}_4)$ (for the fourth regime) can be either triangular or "full" depending on the specific model under consideration. Consequently, these structures allow for the possibility of modeling endogeneity and reverse causality phenomena.

The SVAR thus identified generates regime-dependent IRFs. Let $A_i, i = 1, 2, 3, 4$, be the reduced-form companion matrices associated with the system in Equation 9. The dynamic response of X_{t+h} to a one-standard-deviation shock in variable j at time t is summarized by the (population) IRFs:

$$\text{IRF}_j(h) := \begin{cases} R'(A_1)^h R\tilde{B}_j, & t \leq T_{B_1}, \\ R'(A_2)^h R(\tilde{B}_j + \tilde{Q}_{2j}), & T_{B_1} < t \leq T_{B_2}, \\ R'(A_3)^h R(\tilde{B}_j + \tilde{Q}_{2j} + \tilde{Q}_{3j}), & T_{B_2} < t \leq T_{B_3}, \\ R'(A_4)^h R(\tilde{B}_j + \tilde{Q}_{2j} + \tilde{Q}_{3j} + \tilde{Q}_{4j}), & t > T_{B_3}, \end{cases} \tag{19}$$

where R is still a selection matrix, $\tilde{B}_j, \tilde{Q}_{2j}$, $\tilde{Q}_{3j}$ and $\tilde{Q}_{4j}$ are the j-th columns of $\tilde{B}, \tilde{Q}_2$, $\tilde{Q}_3$ and $\tilde{Q}_4$, respectively.

2.4 Integrating the First Approach as a Particular Instance of the Second Method

Consider a SVAR identified through heteroskedasticity, as in Bacchiocchi and Fanelli (2015), assuming two volatility regimes for simplicity (though the approach can be extended to more than two regimes). Under these conditions, we have:

$$\Sigma_{u,1} = BB'$$

$$\Sigma_{u,2} = (B + Q_2)(B + Q_2)'$$

Now consider the method proposed by Lanne and Lütkepohl (2008), where Λ_1 is normalized to the identity matrix:

$$\Sigma_{u,1} = BB'$$

$$\Sigma_{u,2} = B\Lambda_2 B'$$

If we apply that $Q_2 = B(\Lambda_2^{1/2} - I_n)$ [3] we get that:

$$\begin{aligned}
&(B + B(\Lambda_2^{1/2} - I_n))(B + B(\Lambda_2^{1/2} - I_n))' = \\
&(B + B\Lambda_2^{1/2} - B)(B + B\Lambda_2^{1/2} - B)' = \\
&(B\Lambda_2^{1/2})(B\Lambda_2^{1/2})' = B\Lambda_2^{1/2}(\Lambda_2^{1/2})'B' = \\
&B\Lambda_2 B'
\end{aligned}$$

This demonstrates that the approach used by Lanne and Lütkepohl (2008) is a special case of the methodology applied here.

For a final demonstration, we consider the most general case, allowing for structural parameters to change across volatility regimes while also permitting the variance matrix of structural shocks in the second regime to differ from the identity matrix, though still remaining diagonal:

$$\Sigma_{u,1} = BB'$$
$$\Sigma_{u,2} = (B + Q_2)\Lambda_2(B + Q_2)'$$

In which the difference $\Sigma_{u,1} \neq \Sigma_{u,2}$ is (apparently) explained either by the change in the variance of the structural shocks ε_t before ($\Lambda_1 = I_n$) and after ($\Lambda_2 \neq I_n$) the break, or by the different impact of the shocks across volatility regimes if $Q_2 \neq 0_{n\times n}$, or, possibly, by a combination of these two factors. In Bacchiocchi, E., & Fanelli, L. (2015) it is demonstrated that for every Q_2 and any given $\Lambda_2 \neq I_n$, one can always find a matrix Q_2^* such that the equality

$$(B + Q_2)\Lambda_2(B + Q_2)' = (B + Q_2^*)(B + Q_2^*)'$$

is respected, where

$$Q_2^* = (B + Q_2)\Lambda_2^{1/2} - B.$$

This means that any situation with an apparent change in the volatilities of the structural shocks across regimes can be rewritten as one in which the volatility of the structural shocks remains constant (and normalized to the identity matrix I_n), and only the structural parameters change (via the Q_2 matrix). Also in this case the demonstration can be applied with a number of regimes greater than two.

3 Empirical Results

In this section, we apply the SVAR for $X_t := (U_{Mt}, Y_t, U_{Ft})'$ presented in and discussed in the previous section to address our two main research questions:

1. How does the response of Y_t to shocks in (U_{Mt}, U_{Ft}) vary across macroeconomic regimes?
2. Are U_{Mt} and U_{Ft} exogenous drivers of Y_t, or do U_{Mt} and U_{Ft} respond endogenously to shocks in Y_t?

Section 3.1 introduces the dataset used in our analysis, while Section 3.2 examines the evidence supporting the existence of four distinct volatility regimes. In Section 3.3, we outline and discuss the baseline nonrecursive SVAR specification. Finally, Section 3.4 evaluates the exogeneity of uncertainty and Section 3.5 explores the corresponding impulse response functions (IRFs).

3.1 Data

The dataset used to implement our baseline VAR consists of the variables $X_t := (U_{Mt}, Y_t, U_{Ft})'$, where U_{Mt} represents macroeconomic uncertainty, Y_t is a measure of real economic activity proxied by the growth rate of real industrial production, and U_{Ft} denotes financial uncertainty. The data for Y_t is sourced from the FRED database, while the two uncertainty indices are obtained from Sydney C. Ludvigson's database. The variables are monthly and span the sample 1960:M08-2024:M06 for a total of T = 767 observations. In Jurado et al., *Measuring Uncertainties* (2015) it is explained how the indexes for uncertainties are computed. In particular let us define h-period ahead uncertainty in the variable $y_{jt} \in Y_t = (y_{1t}, \ldots, y_{N_y t})'$, denoted by $U_{jt}^y(h)$, to be the conditional volatility of the purely unforecastable component of the future value of the series. Specifically,

$$U_{jt}^y(h) \equiv \sqrt{E\left[(y_{jt+h} - E[y_{jt+h}|\mathcal{I}_t])^2 \,\middle|\, \mathcal{I}_t\right]}, \tag{20}$$

[3] For a number of regimes greater than two, Q_i with $i > 2$ can be expressed as:

$$Q_i = B(\Lambda_i^{1/2} - \Lambda_{i-1}^{1/2})$$

where the expectation $E(\cdot|\mathcal{I}_t)$ is taken with respect to information $\mathcal{I}_t$ available to economic agents at time t. If the expectation today (conditional on all available information) of the squared error in forecasting y_{jt+h} rises, uncertainty in the variable increases. The accurate measurement of uncertainty necessitates removing the forecastable component $E[y_{jt+h} \mid \mathcal{I}_t]$ before calculating conditional volatility. Failure to do so results in estimates that mistakenly classify forecastable variations as "uncertain." Therefore, uncertainty in a series is not equivalent to the conditional volatility of the raw series; instead, it is crucial to eliminate the entire forecastable component.

A measure, or index, of *macroeconomic uncertainty* can then constructed by aggregating individual uncertainty at each date using weights w_j.

$$U_t^y(h) := \lim_{N_y \to \infty} \sum_{j=1}^{N_y} w_j U_{jt}^y(h)$$

Macroeconomic uncertainty is not equal to the uncertainty in any single series y_{jt}. Instead, it represents a measure of the common variation in uncertainty across many series.

3.2 Identification of volatility regimes

To provide evidence of the existence of multiple volatility regimes in the variance-covariance matrix of the VAR innovations, we followed the methodology outlined in Angelini, Bacchiocchi, Caggiano, and Fanelli (2018). Specifically, we estimated a VAR model with $p = 4$ lags for the variables under consideration using different estimation windows. We employed a rolling window estimation of 10 years, another of 15 years, and a recursive estimation window starting with an initial sample of 10 years. The values of Σ_u were then computed, and the non-redundant elements were plotted in Figure 3 to visually identify the primary structural breaks in the time series. The graphs on the diagonal report the estimated variances, while the off-diagonal terms report the estimated covariances for the recursive (blue line), the 10-year (red line), and the 15-year (orange line) rolling windows VARs.

The vertical dashed lines correspond to the potential break dates that define the different volatility regimes. These dates are $T_{B1} = 1984{:}M3$, $T_{B2} = 2007{:}M12$, and $T_{B3} = 2019{:}M11$. The three break dates partition the entire sample period from 1960:M8 to 2024:M6 into four distinct subsamples: the Great Inflation period (1960:M8–1984:M3, $T = 280$), the Great Moderation period (1984:M4–2007:M12, $T = 285$), the Great Recession + Slow Recovery period (2008:M1–2019:M11, $T = 143$), and the COVID-19 + Recovery period (2019:M12–2024:M6, $T = 55$).

As highlighted in the previous studies, the graph clearly demonstrates that the average volatility level is time-varying. Volatility was higher during the 1970s and 1980s, declined steadily from the mid-1980s to the end of 2007, and then increased again after the financial crisis of 2007–08, before stabilizing.

The key contribution of this paper, however, lies in the observation that after the stabilization in the third regime, there was a sharp increase in all variances and covariances during the months when COVID-19 began to significantly impact the global economy. This prompted the testing of dates corresponding to the months prior to this unprecedented shock. Our findings indicate that November 2019 (2019:M11) is the date most consistently supported by statistical tests, thereby justifying the introduction of a fourth regime. Interestingly, this date not only marks the beginning of the fourth regime but also coincides with the onset of the COVID-19 pandemic in China. Despite its geographical distance from the U.S., the outbreak began to escalate global uncertainty and fear.

The types of tests we employed include Chow-type tests to verify the joint null hypothesis H_0 that there are no breaks in the VAR coefficients: the covariance matrices of residuals and the autoregressive parameters.

$$H_0 : (\Pi_1 \quad \Sigma_{u,1}) = (\Pi_2 \quad \Sigma_{u,2}) = (\Pi_3 \quad \Sigma_{u,3}) = (\Pi_4 \quad \Sigma_{u,4}) = (\Pi \quad \Sigma_u) \tag{21}$$

Additionally, we utilized a Chow-type test to assess the null hypothesis H_0', which posits the absence of structural breaks in Σ_u, indicating no volatility regimes, while holding the autoregressive parameters constant: $\Pi_1 = \Pi_2 = \Pi_3 = \Pi_4 = \Pi$.

$$H_0' : \Sigma_{u,1} = \Sigma_{u,2} = \Sigma_{u,3} = \Sigma_{u,4} = \Sigma_u \tag{22}$$

These tests are detailed in Table 1. The findings indicate a strong rejection of the null hypothesis H_0, as demonstrated by a log-likelihood ratio (LR) test statistic of 796.95, which is highly significant with a P-value of 0.000, according to the $\chi^2(135)$ distribution. Similarly, the computed LR test for H_0' also decisively rejects the null hypothesis, yielding a test statistic of 419.7 with a P-value of 0.000, derived from the $\chi^2(18)$ distribution. As previously illustrated in Figure 3, these results confirm that the unconditional variances and covariances have varied over time. This analysis not only confirms the presence of four distinct volatility regimes within the data but also offers preliminary insights into the evolving dynamics between the measures of uncertainty, U_{Mt} and U_{Ft}, and real economic activity, Y_t. These insights will guide the development of the structural framework in the subsequent section.

Additionally, Table 1 summarizes some diagnostic statistics associated with the estimated models. These statistics suggest that the VAR residuals are not Gaussian, although they do not exhibit serial correlation within regimes. In summary, the fitted reduced-form model for $X_t = (U_{Mt}, Y_t, U_{Ft})'$ aligns well with the observed data. This model is in fact deemed a robust reduced-form version of the nonrecursive SVAR that will be detailed later.

3.3 Identification Restrictions

In this section, we introduce the specification of the matrices of the structural parameters: $\tilde{B} = B(\theta)$, $\tilde{Q}_2 = Q_2(\theta)$, $\tilde{Q}_3 = Q_3(\theta)$, and $\tilde{Q}_4 = Q_4(\theta)$ which fulfill the identification conditions. The analysis for the first three regimes closely follows the approach of Angelini G., Bacchiocchi E., Caggiano G., and Fanelli L. (2018). An analysis of the estimated correlation values in Table 1 reveals that the correlation between macroeconomic uncertainty and real economic activity is lower during the Great Moderation regime, higher during the Great Inflation, and even higher in the third regime of the Great Recession + Slow Recovery period. This indicates that the impact of macroeconomic uncertainty is highly regime-dependent. However, these correlation values alone do not allow us to infer causality; thus, we cannot definitively state whether it is macroeconomic factors that cause economic activity, the reverse, or both.

Financial uncertainty only begins to negatively correlate with real economic activity in the third regime, though this parameter is not statistically significant at the 10% level. Since financial uncertainty is largely uncorrelated with real activity, its impact on the business cycle, if any, likely manifests through its correlation with macroeconomic uncertainty. This correlation is almost negligible in the initial subsample and only increases significantly after the mid-1980s. Specifically, the correlation between the residuals associated with macroeconomic and financial uncertainty equations increases substantially across the four volatility regimes—from 12%, to 32%, to 48%, and finally to 72%. This pattern suggests that while the two sources of uncertainty were relatively independent during the Great Inflation period, they have become much more correlated thereafter, particularly during periods of financial turmoil. From the fourth period onward, u_{Ft} starts to also have a significant correlation with real economic activity. This shift underscores the growing importance of financial uncertainty as markets have experienced heightened levels of financial stress.

The main difference in fact emerges in the fourth regime, where we observe that all correlations have consistently become higher, and the estimated values for the uncertainties with respect to economic activity are positive and significant. There are many views and hyphotesis about this fact. This observation aligns with the Growth Option Theory, which posits that higher levels of uncertainty might encourage firms to engage in strategic investments that capitalize on potential high-return opportunities, especially when the downside risks are limited. This behavior is grounded in the concept that uncertainty, characterized by a mean-preserving spread in risk, does not solely pose a threat but also offers a window for significant potential gains. This can be particularly attractive in industries that are innovation-driven or those facing rapid changes. During the pandemic, in fact, technology companies experienced a significant boost, largely due to the acceleration of digital transformation across all sectors of the economy. This surge was fueled by an increased demand for remote working solutions, e-commerce, cloud storage, and online communication platforms, which benefited tech companies substantially.

In contrast, more traditional sectors without a strong digital basis faced significant challenges due to lockdowns, disruptions in physical operations, and decreased consumer spending in non-essential areas. However, the overall economic activity managed to "heal" quite fast thanks to the technology sector's growth, as these companies not only managed to thrive but also supported the continuity of business in other sectors through their services and products. Another key factor in explaining why the residuals associated with economic activity are positively correlated with those of uncertainties is the extreme measures taken by the Federal Reserve and the subsidies provided by the U.S. government after 2020. As it is highlightned in *COVID-19 Uncertainty: A Tale of Two Tails* (2021), during the initial phase of the COVID-19 impact, uncertainty increased significantly alongside a sharp decline in economic activity. As the pandemic progressed, downside risks greatly diminished. By early 2021, while the forecast distribution remained highly dispersed, indicating that subjective uncertainty was still elevated, it increasingly reflected upside rather than downside risks.

In summary, the positive correlation could be due to short-term adaptive measures and investments which temporarily enhance productivity or output. However, as the underlying economic challenges imposed by the pandemic (e.g., supply chain disruptions, ongoing restrictions, consumer sentiment downturns) persist, these gains may not be sustainable in the medium to long term without additional adjustments (see Section 3.5 for the analysis of IRFs).

Based on these considerations we formulate the set of restrictions that we apply to the matrixes of structural parameters. As already stated in Section 2.3, the necessary condition for identification requires imposing at least twelve joint restrictions on the matrices of structural parameters. These restrictions, which can be represented compactly as in Equation 23, must satisfy the necessary and sufficient identification rank condition discussed in Section 2.3; that is, the Jacobian matrix associated with the function in equation (18) must be regular and full column rank.

Great Inflation:

$$\tilde{B} := \begin{pmatrix} b_{\mathrm{MM}} & 0 & 0 \\ b_{\mathrm{YM}} & b_{\mathrm{YY}} & 0 \\ 0 & 0 & b_{\mathrm{FF}} \end{pmatrix};$$

Great Moderation:

$$\tilde{B} + \tilde{Q}_2 := \begin{pmatrix} b_{\mathrm{MM}} + q_{2,\mathrm{MM}} & 0 & q_{2,\mathrm{MF}} \\ b_{\mathrm{YM}} + q_{2,\mathrm{YM}} & b_{\mathrm{YY}} + q_{2,\mathrm{YY}} & 0 \\ 0 & 0 & b_{\mathrm{FF}} + q_{2,\mathrm{FF}} \end{pmatrix};$$

Great Recession + Slow Recovery:

$$\tilde{B}+\tilde{Q}_2+\tilde{Q}_3 := \begin{pmatrix} b_{\text{MM}}+q_{2,\text{MM}} & 0 & q_{2,\text{MF}}+q_{3,\text{MF}} \\ b_{\text{YM}}+q_{2,\text{YM}}+q_{3,\text{YM}} & b_{\text{YY}}+q_{2,\text{YY}}+q_{3,\text{YY}} & q_{3,\text{YF}} \\ q_{3,\text{FM}} & 0 & b_{\text{FF}}+q_{2,\text{FF}}+q_{3,\text{FF}} \end{pmatrix};$$

COVID-19 + Recovery:

$$\tilde{B}+\tilde{Q}_2+\tilde{Q}_3+\tilde{Q}_4 := \begin{pmatrix} b_{\text{MM}}+q_{2,\text{MM}}+q_{4,\text{MM}} & q_{4,\text{MY}} & q_{2,\text{MF}}+q_{3,\text{MF}}+q_{4,\text{MF}} \\ b_{\text{YM}}+q_{2,\text{YM}}+q_{3,\text{YM}} & b_{\text{YY}}+q_{2,\text{YY}}+q_{3,\text{YY}}+q_{4,\text{YY}} & q_{3,\text{YF}}+q_{4,\text{YF}} \\ q_{3,\text{FM}} & 0 & b_{\text{FF}}+q_{2,\text{FF}}+q_{3,\text{FF}}+q_{4,\text{FF}} \end{pmatrix} \tag{23}$$

The specification of the matrices $\tilde{B}$ and $\tilde{Q}_2$ follows the framework established by Angelini et al. (2018), as it has been rigorously tested. Specifically, we assume that during the Great Inflation period, financial uncertainty is exogenous on impact with respect to structural shocks from macroeconomic uncertainty and real activity ($b_{FM} = b_{FY} = 0$). Additionally, it is assumed that financial uncertainty does not exert contemporaneous effects on macroeconomic uncertainty, denoted as $b_{MF} = 0$.

Moreover, we have restricted the direct influence of financial uncertainty on real economic activity to zero ($b_{YF} = 0$). This decision is based on the heavily regulated financial markets prior to the 1980s, a period followed by deregulation that granted easier access to financial liquidity for households and firms. This regulatory environment slowed the responsiveness of financial markets to non-financial dynamics and vice versa. In the second regime, financial uncertainty is still expected to react to and impact real economic activity with lags ($q_{2,FY} = q_{2,YF} = 0$). We now permit it to influence macroeconomic uncertainty at the moment of the shock ($q_{2,MF} \neq 0$), as inferred from estimated correlations in Table 1.

The causality relationships considered in the third regime suggest that macroeconomic uncertainty responds with the same magnitude to its own structural shocks[4]. The remainder is the same as in the Great Moderation period, except for two newly estimated free parameters, $q_{3,FM}$ and $q_{3,YF}$. Leaving these two parameters unrestricted enables us to test whether periods of high financial stress have made financial uncertainty respond on impact to macroeconomic uncertainty shocks compared to previous regimes (and so to infer whether the increased correlation between U_{Mt} and U_{Ft} observed during the Great Recession + Slow Recovery relative to the Great Moderation can be ascribed to financial or macro uncertainty shocks, or to both types of shocks), and to permit for a direct impact of financial uncertainty on real economic activity, respectively. Finally, the matrix $\tilde{Q}_4$, capturing the transition from the third to the COVID-19 + Recovery period, necessitated some specific adjustments. We decided to set the parameters q_{4YM}[5], q_{4FM}, and q_{4FY} to zero. A novel aspect in comparison to other matrices is that we left the parameter q_{4MY} unrestricted, allowing for a direct influence of real activity on macroeconomic uncertainty. This decision considers the unique and extraordinary dynamics observed in the fourth regime of this analysis, where a sharp decline in economic activity could potentially initiate a negative spiral with macroeconomic uncertainty. Maintaining q_{4FY} as zero aligns with our theoretical perspective of financial uncertainty being exogenous relative to economic activity. Although the COVID-19 crisis primarily stemmed from health sector disruptions, making it an "economic" crisis, financial uncertainty often preceded decreases in real economic activity (see Figure 2). This observation supports our model specification where both uncertainties may influence each other, yet financial uncertainty does not respond immediately to shocks in real economic activity.

The nonrecursive SVAR specified in Equation 23 is estimated over the period from 1960:M8 to 2024:M6, imposing four volatility regimes associated with the three break dates: $TB1 = 1984:M3$, $TB2 = 2007:M12$, and $TB3 = 2019:M11$. The (quasi-)maximum likelihood estimates of the structural parameters γ that enter the matrices $\tilde{B}$, $\tilde{B}+\tilde{Q}_2$, $\tilde{B}+\tilde{Q}_2+\tilde{Q}_3$, and $\tilde{B}+\tilde{Q}_2+\tilde{Q}_3+\tilde{Q}_4$ are reported for $h = 1$ (1-month horizon uncertainty) in Table 2. The second row of Table 2 refers to the specification in Equation 23, while the third row refers to the same model estimated with the additional constraints $q_{3FM} = q_{4MY} = 0$. The first row represents the "endogenous" specification used by Angelini G., Bacchiocchi E., Caggiano G., and Fanelli L. (2018) to support the thesis of the exogeneity of macroeconomic and financial uncertainty with respect to economic activity. The estimated structural parameters $\hat{\gamma}$ in Table 2 correspond to the on-impact responses featured by our Impulse Response Functions (IRFs).

We first discuss the issue of reverse causality and exogeneity; then we analyze the dynamic causal effects as implied by the estimated IRFs.

3.4 Reverse causality/endogeneity and main specification

Thanks to Table 2, we can address the principal questions of this paper: considering the newly identified fourth regime of volatility, we examine whether macroeconomic uncertainty is exogenous or responds on impact to unexpected structural changes in real economic activity, and whether financial uncertainty is directly caused by unexpected structural shocks in macroeconomic uncertainty. The analysis confirms that all three specifications align with the data; however, further

[4]Considering the extension of the dataset to include the period from 2015:M4 to 2019:M11 into the third regime, differing from Angelini G., Bacchiocchi E., Caggiano G., and Fanelli L. (2018), the parameter q_{3MM} of $\tilde{Q}_3$ was initially left unconstrained. This resulted in a deterioration of the estimated log-likelihood and the parameter $\tilde{B}+\tilde{Q}_2+\tilde{Q}_3(1,1)$ was found to be statistically insignificant. Consequently, we have decided to retain the restriction of q_{3MM} to zero, consistent with the methodology established in the cited paper.

[5]Similar to the approach with q_{3MM}, q_{4YM} was initially estimated without constraints. However, upon determining the statistical insignificance of $\tilde{B}+\tilde{Q}_2+\tilde{Q}_3+\tilde{Q}_4(2,1)$ at the 5% level, we imposed a zero restriction, which also improved the fit of the structural model.

deliberations are warranted. The second row of Table 2 displays the estimates for the matrices of structural parameters as specified in Equation 23. The likelihood ratio test for the three overidentification restrictions results in a statistic of 7.1757, with associated P-value of 0.0665, suggesting that the identification restrictions are statistically acceptable, although the confidence interval is not wide. Notably, the parameters $\tilde{B}+\tilde{Q}_2+\tilde{Q}_3(3,1)$ and $\tilde{B}+\tilde{Q}_2+\tilde{Q}_3+\tilde{Q}_4(1,2)$ do not achieve significance at the 5% level. Proper statistical procedures may warrant restricting q_{3FM} and q_{4MY} to zero. This is why we decided to test a set of restrictions where these last two parameters were set to zero, as detailed in the specification in the third row of Table 2. With this model, all parameters for $\tilde{B}+\tilde{Q}_2+\tilde{Q}_3$ and $\tilde{B}+\tilde{Q}_2+\tilde{Q}_3+\tilde{Q}_4$ became significant, except for $\tilde{B}+\tilde{Q}_2+\tilde{Q}_3(2,3)$. Importantly, we verified that $\tilde{B}+\tilde{Q}_2+\tilde{Q}_3(2,3)$, although not statistically significant, still provides relevant information about the relationship between financial uncertainty and real economic activity. Imposing $q_{3YF}=0$, in fact, would significantly deteriorate the model's fit and contradict the theoretical analysis suggesting a potential negative direct effect of financial uncertainty on real economic activity, particularly following the relaxation of stringent regulations in the 1980s (see Ng and Wright (2013)). With this setup, the log-likelihood ratio test for the five overidentification restrictions yielded a statistic of 7.4953, with an associated p-value of 0.1863, indicating greater acceptance compared to the model where macroeconomic uncertainty was treated as "endogenous" in the fourth regime and allowed to influence instantaneously financial uncertainty from the third regime onwards. In fact, the log-likelihood ratio test comparing the model in the third row against the one in the second shows a statistic of 0.3195, with an associated p-value of 0.8523. From these results, we can confidently assert that macroeconomic uncertainty remains exogenous even during the period starting from the COVID-19 pandemic. Additionally, financial uncertainty is not significantly affected by shocks from macroeconomic uncertainty upon impact. During the Great Recession + Slow Recovery period, although the two sources of uncertainty appear increasingly correlated, the direction of this correlation seems to remain consistent across different regimes.

It could be argued that while the exogeneity of macroeconomic uncertainty with respect to economic activity has been tested, the same is not true for financial uncertainty, which is assumed to be exogenous across all specifications. For this reason, we reversed the positions of U_{Mt} and U_{Ft} in the vector $X_t := (U_{Mt}, Y_t, U_{Ft})'$ and estimated a SVAR using the set of restrictions presented in Equation 23. This adjustment leads to a radical change in the roles played by the two sources of uncertainty within the system. The likelihood ratio test statistic for the three overidentification restrictions is 26.9893, with an associated p-value of 5.9179e-06, strongly rejecting the model. We interpret this result as evidence of the distinct roles that the two indices of uncertainty play in the system.

The final test compares the current specification with the one also tested by Angelini et al. (2018). This model is presented on the first row of Table 2. Specifically, this specification mirrors the main "exogenous" model presented in the third row of Table 2, except that the parameters b_{MY} and q_{2FM} are freely estimated. Not restricting these two parameters to zero permits "endogenous" macroeconomic uncertainty beginning with the first regime, and allows for the possibility that macroeconomic uncertainty shocks might trigger financial uncertainty. This approach does not preclude a bidirectional structural relationship between uncertainties, instead it suggests its potential from the second regime onward.

Surprisingly, this set of restrictions is not entirely rejected by the data, as evidenced by a log-likelihood ratio test statistic of 6.9976, with an associated p-value of 0.0720. However, when comparing the main "exogenous" specification against this alternative, the test yields a statistic of 0.4977 with a p-value of 0.779, indicating that the null hypothesis favoring the "exogenous" specification, cannot be rejected, aligning with the findings of Angelini et al. (2018).

Therefore, the main specification validated by the data is the one outlined in Equation 24.

Great Inflation:

$$\tilde{B} := \begin{pmatrix} b_{\mathrm{MM}} & 0 & 0 \\ b_{\mathrm{YM}} & b_{\mathrm{YY}} & 0 \\ 0 & 0 & b_{\mathrm{FF}} \end{pmatrix};$$

Great Moderation:

$$\tilde{B}+\tilde{Q}_2 := \begin{pmatrix} b_{\mathrm{MM}}+q_{2,\mathrm{MM}} & 0 & q_{2,\mathrm{MF}} \\ b_{\mathrm{YM}}+q_{2,\mathrm{YM}} & b_{\mathrm{YY}}+q_{2,\mathrm{YY}} & 0 \\ 0 & 0 & b_{\mathrm{FF}}+q_{2,\mathrm{FF}} \end{pmatrix};$$

Great Recession + Slow Recovery:

$$\tilde{B}+\tilde{Q}_2+\tilde{Q}_3 := \begin{pmatrix} b_{\mathrm{MM}}+q_{2,\mathrm{MM}} & 0 & q_{2,\mathrm{MF}}+q_{3,\mathrm{MF}} \\ b_{\mathrm{YM}}+q_{2,\mathrm{YM}}+q_{3,\mathrm{YM}} & b_{\mathrm{YY}}+q_{2,\mathrm{YY}}+q_{3,\mathrm{YY}} & q_{3,\mathrm{YF}} \\ 0 & 0 & b_{\mathrm{FF}}+q_{2,\mathrm{FF}}+q_{3,\mathrm{FF}} \end{pmatrix};$$

COVID-19 + Recovery:

$$\tilde{B}+\tilde{Q}_2+\tilde{Q}_3+\tilde{Q}_4 := \begin{pmatrix} b_{\mathrm{MM}}+q_{2,\mathrm{MM}}+q_{4,\mathrm{MM}} & 0 & q_{2,\mathrm{MF}}+q_{3,\mathrm{MF}}+q_{4,\mathrm{MF}} \\ b_{\mathrm{YM}}+q_{2,\mathrm{YM}}+q_{3,\mathrm{YM}} & b_{\mathrm{YY}}+q_{2,\mathrm{YY}}+q_{3,\mathrm{YY}}+q_{4,\mathrm{YY}} & q_{3,\mathrm{YF}}+q_{4,\mathrm{YF}} \\ 0 & 0 & b_{\mathrm{FF}}+q_{2,\mathrm{FF}}+q_{3,\mathrm{FF}}+q_{4,\mathrm{FF}} \end{pmatrix} \tag{24}$$

Previous studies such as those by Ludvigson et al. (2018a) and Carriero et al. (2018b) have investigated the exogeneity and endogeneity of uncertainty. Our findings align with Ludvigson et al. (2018a), supporting the view that financial uncertainty is largely exogenous to the business cycle. According to our identification scheme, financial uncertainty impacts the business cycle indirectly by initially triggering macroeconomic uncertainty, although this real effect becomes also direct in the fourth period. Conversely, while our results diverge from those of Ludvigson et al., they are consistent with Carriero et al. (2018b), providing strong evidence that macroeconomic uncertainty exerts an exogenous influence on the business cycle.

Carriero et al. (2018b) employed a stochastic volatility approach within VARs to simultaneously assess the impacts of macroeconomic and financial uncertainties, alongside real economic activity, without distinguishing the discrete effects of each uncertainty type. This approach underlines the necessity of integrating both macroeconomic and financial uncertainty indices to accurately discern their relationship with real economic activity, as these indices exhibit distinctly different characteristics.

Ludvigson et al. (2018a) introduced an innovative identification strategy within a static framework to simultaneously identify the shocks of uncertainty and real activity without imposing constraints on their contemporaneous interactions. This method utilizes shock-based restrictions, such as event and correlation constraints, which mandate significant responses during major financial disruptions (e.g., the 1987 stock market crash and the 2007–09 financial crisis) and leverage external instruments to refine shock identification. The endogeneity of macroeconomic uncertainty they document might reflect the "asymmetric" characterization of financial and macroeconomic uncertainty shocks implicit in their approach—that is, the fact that the "event constraints" are imposed mainly on financial uncertainty.

Similar to Ludvigson et al. (2018a), our analysis indicates a significantly positive immediate impact of macroeconomic uncertainty on real activity, but only during the fourth regime. Additionally, our results reveal that financial uncertainty also contributes positively to this immediate effect, marking a departure from the findings of Ludvigson et al. (2018a) (see the Sections 3.3 and 3.5 for an explanation of those positive estimated values). Finally, by examining Figures 4-5, we observe that while the structural shocks identified in our analysis—ε_{Mt}, ε_{Yt}, ε_{Ft}—do not directly correspond to the primitive shocks of any specific model, as they can emanate from various "macroeconomic," "real activity," and "financial" sources, it is evident that the estimated shocks are systematically higher during NBER-identified recession periods (indicated by the shaded areas in the graphs). The graphs also reveal distinct differences between macro and financial uncertainty shocks. Notably, significant macro uncertainty shocks correlate with the oil price shocks of the 1970s, whereas the 1987 stock market crash serves as a prime example of a major financial uncertainty shock that did not lead to an increase in macroeconomic uncertainty. The Global Financial Crisis of 2007-2009 and COVID-19 pandemic of 2020, however, are two notable instances where both macroeconomic and financial uncertainties escalated significantly, coinciding with sharp declines in real economic activity. Interestingly, the identified financial uncertainty shocks align with the 'event constraints' described by Ludvigson et al. (2018).

3.5 IRFs

Considering the approach specified in Equation 19, we proceed by computing the Impulse Response Functions (IRFs) for each regime and for the model in Equation 24 by replacing A_1, A_2, A_3, and A_4, and $\tilde{B}$, $\tilde{B}+\tilde{Q}_2$, $\tilde{B}+\tilde{Q}_2+\tilde{Q}_3$, and $\tilde{B}+\tilde{Q}_2+\tilde{Q}_3+\tilde{Q}_4$ with their estimates presented in Table 2. As previously mentioned, these IRFs differ across volatility regimes because the coefficients of the baseline VAR experience several structural breaks, enabling us to specify the correct set of restrictions for identification. This implies that both the companion matrix and the structural parameters involved in the computation of the IRFs differ across those periods. IRFs are plotted in Figures 6-10 over a horizon of $h = 60$ periods (5 years). Figure 6 plots the IRFs obtained on the four volatility regimes for $h = 1$ (1-month uncertainty). Figures 7-10 plot the IRFs separately for each regime, disentangling the case $h = 1$ (1-month uncertainty) from the case $h = 12$ (1-year uncertainty). All plots show responses to one standard deviation changes in ε_{jt}, $j = M, Y, F$, in the direction that leads to an increase in its own variable X_{it}, $i = M, Y, F$, where $X_{Mt} = U_{Mt}$, $X_{Yt} = Y_t$ and $X_{Ft} = U_{Ft}$, respectively. This normalization allows us to directly compare the responses of real economic activity in the four volatility regimes. In Figure 6, the blue IRFs refer to the Great Inflation period, the red IRFs to the Great Moderation period, the yellow IRFs to the Great Recession + Slow Recovery period, and the purple IRFs to the COVID-19 + Recovery period. The first row reports the response of macroeconomic uncertainty to the three structural shocks, the second row reports the response of industrial production, and the third row reports the response of financial uncertainty. In this case, confidence bands have not been reported, to ease reading. Table 3 reports the highest negative and significant values of the estimated IRFs, resulting from structural shocks ε_{Yt} or affecting Y_t.

The graphs clearly demonstrate that impulse response functions are strongly regime-dependent. While real economic activity consistently reacts to uncertainty shocks, uncertainty only mildly reacts to real activity shocks. The impact of each shock is notably stronger during the COVID-19 + Recovery period, where moments of financial turmoil and market fear led to increased connectivity between financial and macroeconomic uncertainty and real economic activity. As illustrated in Figures 7-10 and Table 3, the IRFs for uncertainty at a twelve-month horizon are milder and exhibit less noise, suggesting that these indices of uncertainty capture more fundamental information compared to their one-month counterparts. Regarding the last two volatility regimes, over the longer horizon, the impact of financial uncertainty on economic activity tends to diminish, whereas at a one-month horizon, it has a more significant influence on economic outcomes. This is clearly illustrated in Figure 11, which presents the forecast-error variance decomposition for Y_t in the

fourth regime.

In the Great Inflation period, as shown in Figure 7, the response of economic activity to macroeconomic uncertainty is more delayed when the horizon extends to twelve months compared to a one-month horizon, though the effect remains significant for several months. Financial uncertainty shocks are also clearly impactful and significant over an extended period. This aligns with the period's weak monetary policy rule by the Fed, leading to greater fluctuations in economic activity in response to negative shocks.

In contrast, during the Great Moderation period (Figure 8), financial uncertainty seldom significantly impacts real economic activity. Conversely, macroeconomic uncertainty shows a less prominent peak at $h = 1$, yet it becomes more pronounced—but remains of comparable size—when considered over a horizon of $h = 12$, as documented in Table 3. This shift away from the erratic "go-stop" policies of the past, where the Fed often reacted too slowly and weakly to inflationary trends, contributed to reduced macroeconomic volatility and minimized its impact on economic activity by fostering more consistent policy measures.

During the Great Recession + Slow Recovery period, as illustrated in Figure 9, there is a significant decline in economic activity following a positive uncertainty shock, and the responses to both sources of uncertainty exhibit similar declining patterns. Industrial production initially appears resilient but reaches its most significant negative peak after approximately four periods. The magnitude of these peaks, detailed in Table 3, is comparable to those during the Great Inflation period for $h = 1$, but they are substantially larger for $h = 12$. This phenomenon aligns with the Global Financial Crisis's profound impact during a period when policy interest rates were near the zero lower bound, limiting the Fed's ability to use conventional instruments to stabilize the economy. This situation resulted in economic variables becoming more responsive to negative shocks. Additionally, uncertainty exhibits significant negative peaks in response to economic activity shocks two periods after the shocks occur. Unlike previous periods, these effects are significant across both horizons and both indices of uncertainty, providing robust evidence of their validity. While this effect, albeit with a very low magnitude, helps explain why the correlation between uncertainty and real economic activity increases after the GFC, as seen in Table 1, it is insufficient to claim that uncertainty is an endogenous (causal) response to real economic activity shocks, because, according to our analysis, the response is at most lagged one period, but not instantaneous.

In the COVID-19 + Recovery period (Figure 10), all variables seem to respond more strongly but less persistently to structural shocks. In particular, the impact of uncertainty shocks is far more significant in this period. The highest peaks are about five times larger than those estimated for the Great Recession + Slow Recovery period. Interestingly, those peaks occur two to three periods after the shocks, horizon at which the financial uncertainty shock leads to an increase in the contribution in the forecast-error variance of Y_t, as shown in Figure 11. The impact values [6], expectedly estimated positive for both U_{Mt} and U_{Ft}, align with the correlation values estimated in Table 1. As discussed in Section 3.3, this may be attributed to several factors, such as the notion that higher uncertainty implies higher potential returns if we consider limited drawdowns (Growth Option Theory), or the extraordinary measures undertaken by the Fed which prevented economic activity from collapsing due to the Covid shock. The IRFs in Figure 10 illustrate a highly segmented pattern and are characterized by severe overshooting of economic activity (in accordance with Bloom (2009) findings), which then returns to pre-shock values in a stationary but overshooting dynamic. This is consistent with the expected effects of various asset purchase programs and tools that the Fed implemented during these exceptionally challenging times, causing economic activity to respond peculiarly to uncertainty shocks. Referencing the Growth Option Theory, we observe that the broad decline in industrial production may reflect challenges faced by traditional sectors unable to sustain their initial responses or adapt effectively to prolonged uncertainty and evolving market dynamics. Opportunities initially seized may have been depleted, leading to decreased consumer demand and investment, which in turn negatively impacted industrial production.

Castelnuovo et al. (2021) analyze these phenomena by utilizing data from various US production sectors to estimate a hierarchical model with stochastic volatility that incorporates both a common component and sector-specific variations. Their analysis reveals divergent patterns of uncertainty evolution over time across sectors, particularly between durables and nondurables. A VAR analysis, adjusting for aggregate uncertainty, indicates that uncertainty shocks in durables tend to be recessionary, whereas those in nondurables can be expansionary. This underscores the importance of employing sectoral data to grasp the varied dynamics induced by uncertainty shocks across different sectors, often characterized by distinctive non-convex adjustment costs.

3.6 Robustness test

As a final test, we evaluated whether using an alternative proxy for real economic activity would alter the results of this paper. Specifically, we considered $X_t := (U_{Mt}, Y_t, U_{Ft})'$, but where $Y_t = \Delta emp_t$, representing the rate of employment growth in the US. We estimated a SVAR model based on the main specification in Equation 24[7]. The sample spanned from 1960:M8 to 2024:M6, with break dates positioned identically. The results confirm our hypothesis of volatility breaks both in the covariance matrix of VAR innovations and the autoregressive parameters of the VAR. The likelihood ratio test comparing the structural model to the unrestricted one yielded a statistic of 7.7882 with an associated p-value of [0.0997], thus not rejecting the model in this case. This new proxy for real economic activity also corroborates the exogeneity of

[6] $(\hat{B} + \hat{Q}_2 + \hat{Q}_3 + \hat{Q}_4)(2,1)$ and $(\hat{B} + \hat{Q}_2 + \hat{Q}_3 + \hat{Q}_4)(2,3)$ values can be seen in the third row of Table 2

[7] A minor change was made in that the parameter $(\tilde{Q}_4)(2,1)$ was not restricted to zero; however, this modification does not affect any subsequent conclusions

macroeconomic uncertainty and the unidirectional causality from financial to macroeconomic uncertainty. Additionally, the associated IRFs depicted in Figure 12 tend to be qualitatively and quantitatively similar to the ones in Figure 6, although uncertainty appears to respond more strongly to real economic activity during the Great Inflation period, but only several months after the shock and not immediately, as our specification suggests.

4 Conclusions

This paper revisits the impact of macroeconomic and financial uncertainty on the business cycle, extending previous analyses to incorporate the volatile period marked by the COVID-19 pandemic. Building on the foundational work of Angelini et al. (2018) and integrating further insights from the crisis, our research confirms that heightened uncertainty typically contracts real economic activity and tends to escalate during recessions. Notably, the effects of uncertainty shocks are not uniform but vary significantly across different volatility regimes, a dynamic underscored by the pandemic's unique economic challenges.

Our empirical strategy, leveraging a non-recursive SVAR model, allows us to capture these complex dynamics effectively. The appproach that has been used here is the "identification-through-heteroskedasticity". The model's flexibility in handling regime-dependent effects, validated against volatility break dates, confirms the exogenous nature of macroeconomic and financial uncertainty within the business cycle. This finding is rigorously tested, providing robust evidence supporting the distinct roles that macroeconomic and financial uncertainty play in the post-World War II period in the United States. The introduction of a fourth regime to account for the pandemic allows us to explore how unprecedented policy measures and global crises influence economic dynamics, offering fresh insights into the enduring debate on the causal relationships between uncertainty and economic activity. As previously stated, we align with the literature, including Bloom (2009), which argues that uncertainty is an exogenous driver of the business cycle. However, we also acknowledge that financial uncertainty, often driven by non-fundamental factors, tends to precede macroeconomic variables and is not influenced by their structural shocks upon impact. Furthermore, its primary influence on the economy is through fostering greater macroeconomic uncertainty, which then significantly impacts economic activity. To this indirect effect is added also a direct one in the COVID-19 + Recovery period.

In the last identified regime, we also observe a substantially stronger and more significant correlation among all the residuals of the estimated VAR model. This occurs due to the unique characteristics of the period, during which uncertainty reached record levels, amplifying its impact on the economy, as demonstrated in Alfaro, I. N., Bloom, N., & Lin, X. (2018) and Chiara Scotti (2023). However, the use of unconventional monetary policy tools by the Federal Reserve helped prevent economic activity from contracting as much as it otherwise would have. This intervention contributed to a positive correlation between uncertainty and real economic activity.

This positive correlation, along with the various theoretical perspectives discussed in this paper, provides context for the initially positive impact of uncertainty shocks on economic activity. However, as expected, this effect transitions into a negative dynamic impact over time, as illustrated by the impulse response functions (IRFs).

Overall, this paper enriches the existing literature by demonstrating the variable impact of uncertainty shocks over time and across different economic conditions, emphasizing the need for flexible analytical frameworks to accurately assess and respond to evolving economic landscapes.

References

- Alfaro, I. N., Bloom, N., & Lin, X. (2018). The Finance Uncertainty Multiplier. (NBER Working Paper 24571). Cambridge, MA: National Bureau of Economic Research.
- Angelini G, Bacchiocchi E, Caggiano G, Fanelli L. (2018), Uncertainty across volatility regimes. J Appl Econ. 2019;34:437–455.
- Bacchiocchi, E., Castelnuovo, E., & Fanelli, L. (2018). *Gimme a Break! Identification and Estimation of the Macroeconomic Effects of Monetary Policy Shocks in the U.S.* Macroeconomic Dynamics, 22(6), 1613–1651.
- Bacchiocchi E., Fanelli L. (2015), Identification in structural vector autoregressive models with structural changes, with an application to U.S. monetary policy. Oxford Bulletin of Economics and Statistics. 2015;77:761–779.
- Bloom, N. (2009). *The Impact of Uncertainty Shocks*. Econometrica, 77, 623–685.
- Bunn, Philip and Altig, David and Anayi, Lena and Barrero, Jose Maria and Bloom, Nicholas and Davis, Steven J. and Meyer, Brent H. and Mihaylov, Emil and Mizen, Paul and Thwaites, Greg, (November 16, 2021), COVID-19 Uncertainty: A Tale of Two Tails. University of Chicago, Becker Friedman Institute for Economics Working Paper No. 2021-135.
- Carriero, A., Clark, T. E., & Marcellino, M. (2018b). Endogenous Uncertainty. (Working Paper 18/05). Cleveland, OH: Federal Reserve Bank.
- Castelnuovo, E. (2022). Uncertainty before and during COVID-19: a survey. Journal of Economic Surveys.
- Castelnuovo, E., Tuzcuoglu, K., & Uzeda, L. (2021). Sectoral Uncertainty. Bank of Canada and University of Padova, mimeo.
- Chiara Scotti, 2023, Financial Shocks in an Uncertain Economy, Working Papers 2308, Federal Reserve Bank of Dallas.
- Christiano, J. C., Motto, R., & Rostagno, M. (2014). Risk Shocks. American Economic Review, 104, 27–65.
- Jurado K, Ludvigson S. C., Ng S. (2015) Measuring uncertainty. American Economic Review. 2015;105(3):1177–1216.
- Lanne, M., & Lütkepohl, H. (2008). Identifying monetary policy shocks via changes in volatility. Journal of Money, Credit and Banking, 40, 1131–1149.
- Ludvigson, S. C., Ma, S., & Ng, S. (2018a). Uncertainty and business cycles: Exogenous impulse or endogenous response? Unpublished manuscript, draft dated May 9, 2018.
- Ng, S., & Wright, J. H. (2013). Facts and challenges from the Great Recession for forecasting and macroeconomic modeling. Journal of Economic Literature, 51, 1120–1154.
- Qu, Z., & Perron, P. (2007). *Estimating and Testing Structural Changes in Multivariate Regressions*. *Econometrica*, 75(2), 459–502.
- Rigobon, R. (2003). Identification through heteroskedasticity. Review of Economics and Statistics, 85, 777–792.
- Segal, G. (2019). A tale of two volatilities: Sectoral uncertainty, growth, and asset prices. Journal of Financial Economics, 134, 110–140.
- Trujillo-Ortiz, A., R. Hernandez-Walls, K. Barba-Rojo, and L. Cupul-Magana (2007). DorHanomunortest: Doornik-Hansen Omnibus Multivariate (Univariate) Normality Test.

Tables and figures

Figure 1: UM1 and UF1

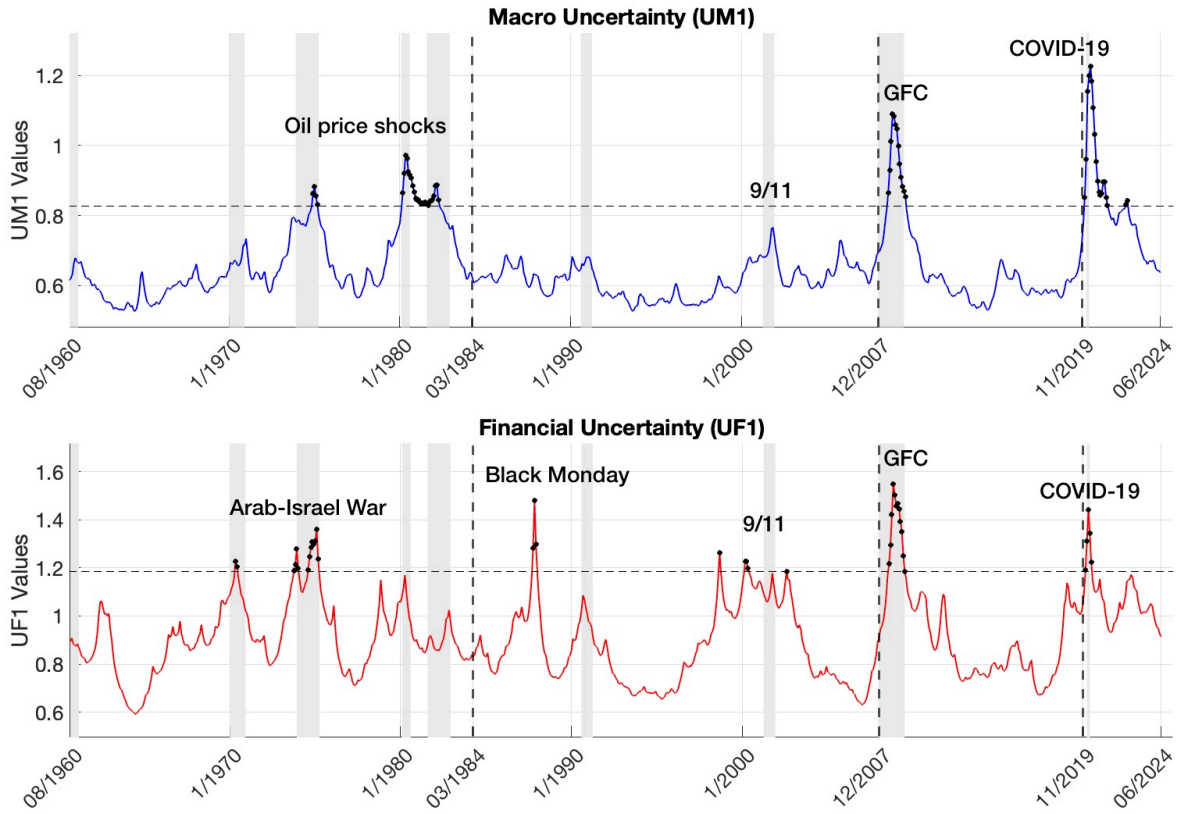

Time series of macro uncertainty U_{Mt} and financial uncertainty U_{Ft}, for an horizon of one month. Shaded areas correspond to NBER recession dates. The horizontal line corresponds to 1.65 standard deviations above the average of each series; the black dots represent months when uncertainty is at least 1.65 standard deviations above the mean.

Figure 2: X_t during the last two regimes

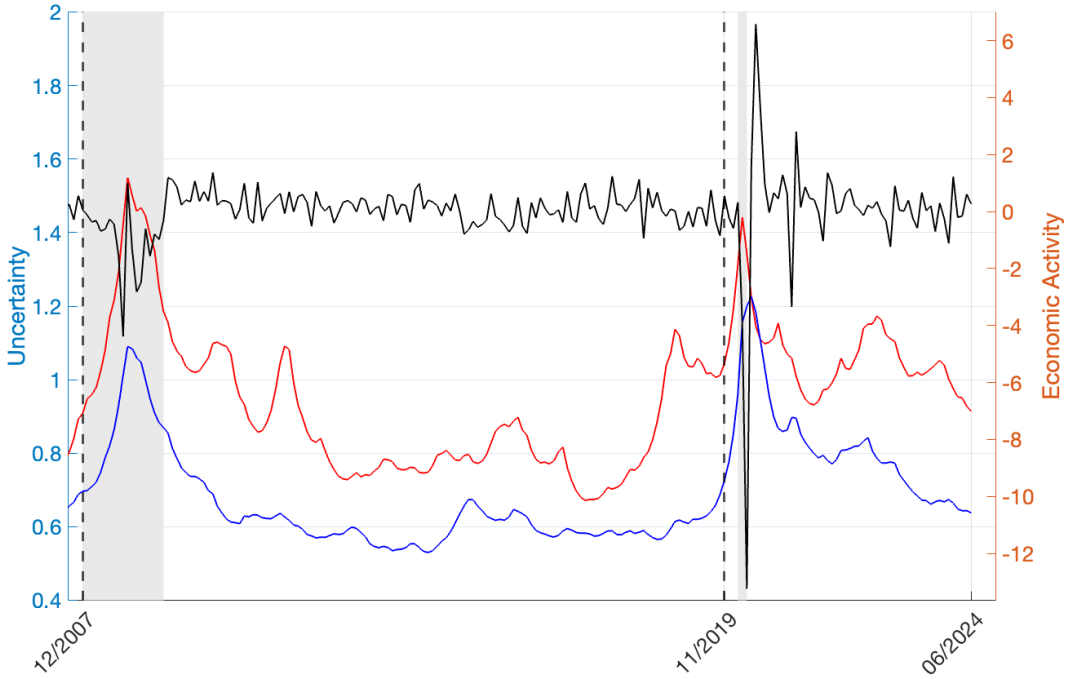

In (red) Financial uncertainty U_{Ft}, in (blue) Macroeconomic uncertainty U_{Mt} both at the horizon of one month. In (black) Economic activity Y_t where $Y_t = \Delta ip_t$ (industrial production growth). The graph includes the Great Recession + Slow Recovery period, 2008:M1–2019:M11, and the Covid-19 + Recovery period, 2019:M12–2024:M6. A double scale is provided for improved visualization.

Figure 3: Error covariance matrix of the VAR

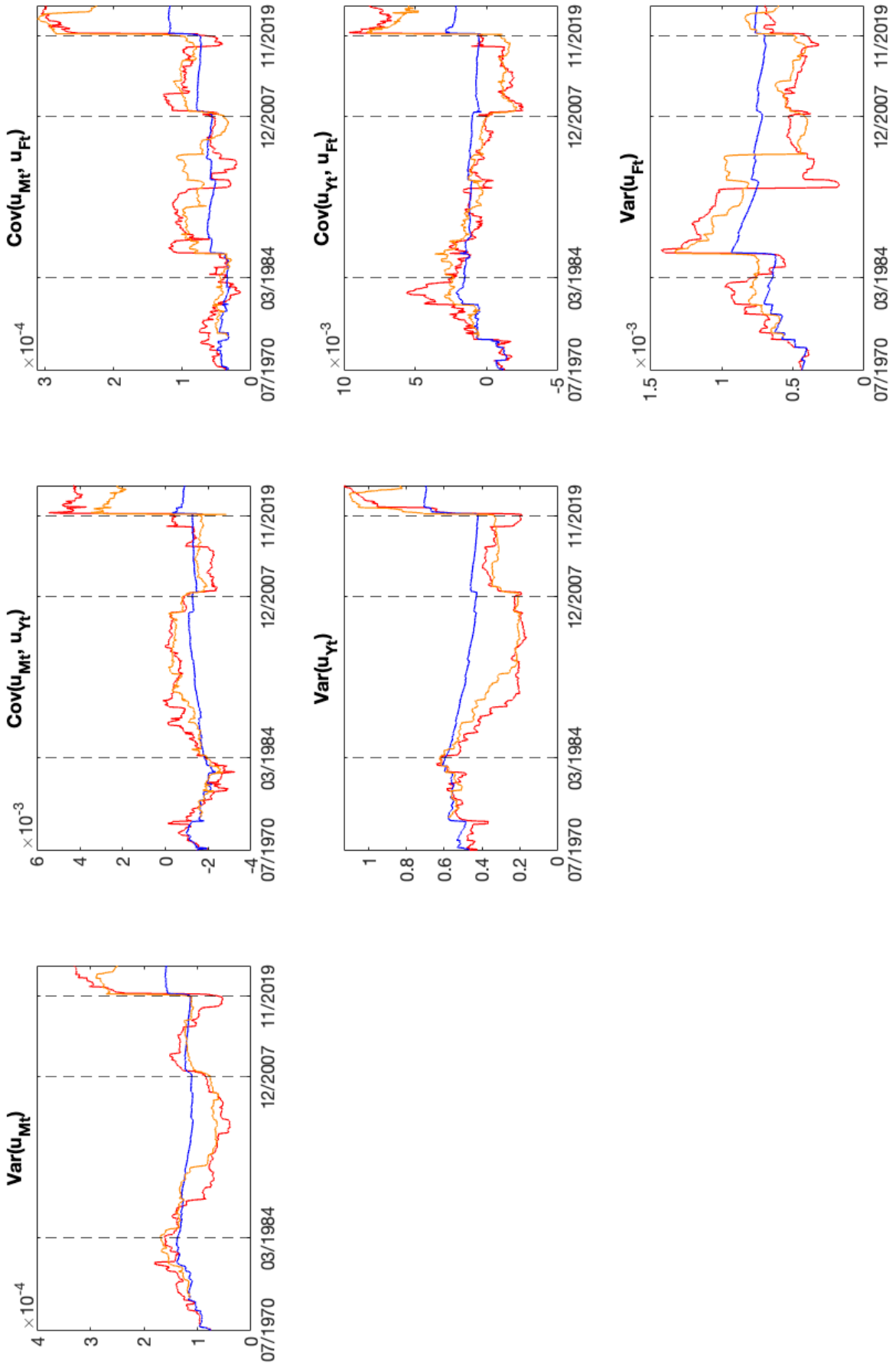

Recursive (blue line), 10-year (red line), and 15-year (orange line) rolling window estimates of the error covariance matrix of the VAR for $X_t := (U_{Mt}, Y_t, U_{Ft})'$, where $Y_t = \Delta ip_t$ (industrial production growth). Dashed black lines denote the three break dates T_{B1} = 1984:$M3$, T_{B2} = 2007:$M12$ and T_{B3} = 2019:$M11$, which separate the four volatility regimes. Overall sample: 1960:M8–2024:M6.

Figure 4: Structural shocks

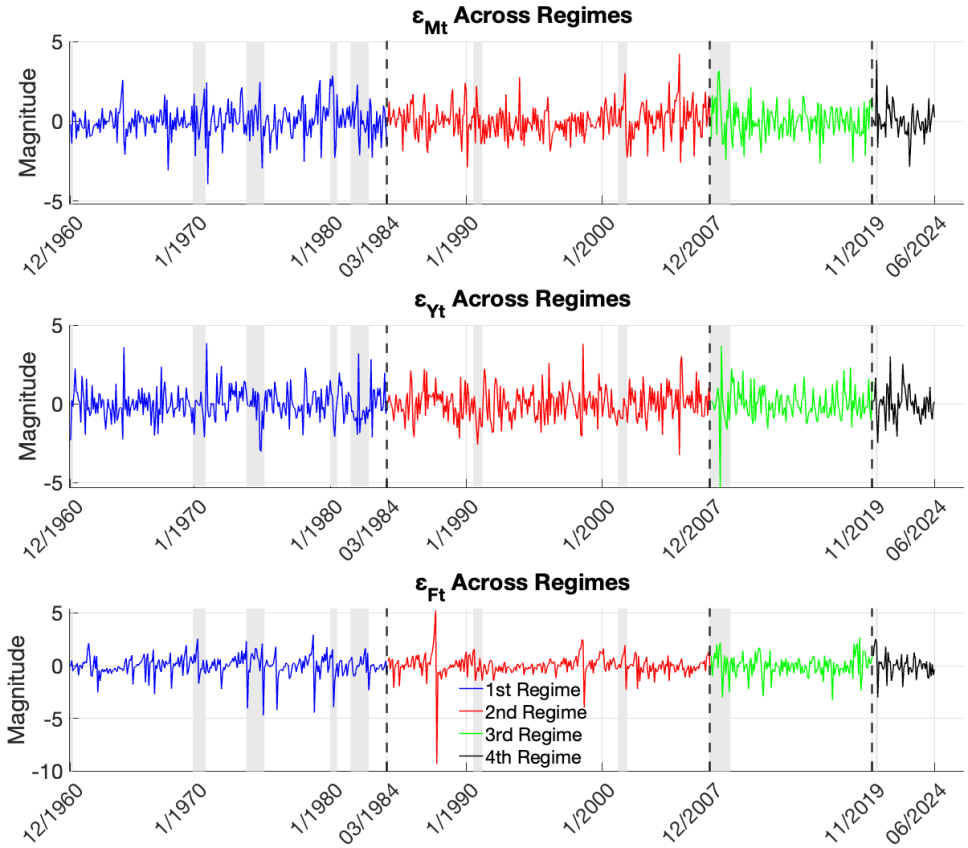

Time series of the structural shocks $\varepsilon_t = B^{-1}u_t$ for the solution of the main specification in Equation 24 applied to $X_t := (U_{Mt}, Y_t, U_{Ft})'$, where $Y_t = \Delta ip_t$ (industrial production growth) and $h = 1$ (1-month uncertainty). The blue line refers to the first volatility regime (Great Inflation, 1960:M8–1984:M3); the red line refers to the second volatility regime (Great Moderation, 1984:M4–2007:M12); the green line refers to the third volatility regime (Great Recession + Slow Recovery, 2008:M1–2019:M11); the black line refers to the fourth volatility regime (COVID-19 + Recovery, 2019:M12–2024:M6).

Figure 5: High magnitude structural shocks

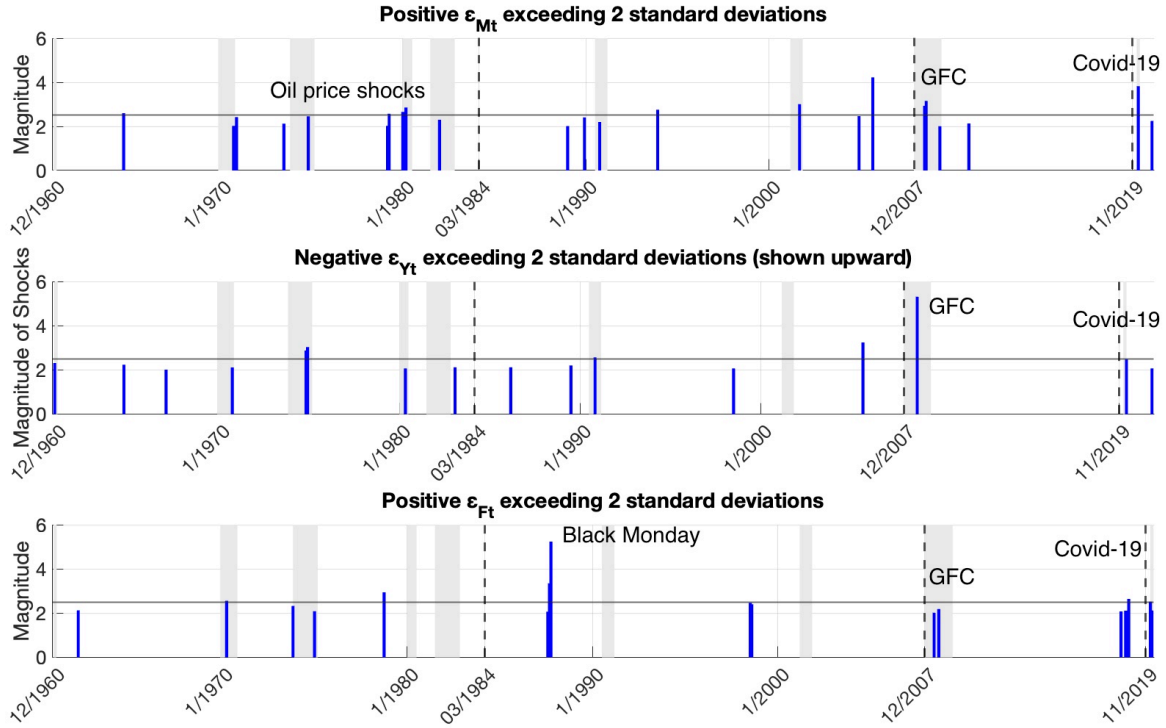

All structural shocks in the identified set that are at least 2 standard deviations above the unconditional mean for ε_{Mt} and ε_{Ft}, and at least 2 standard deviations below the mean for ε_{Yt}. The horizontal line corresponds to 3 standard deviations above/below the unconditional mean of each series.

Figure 6: IRFs across volatility regimes

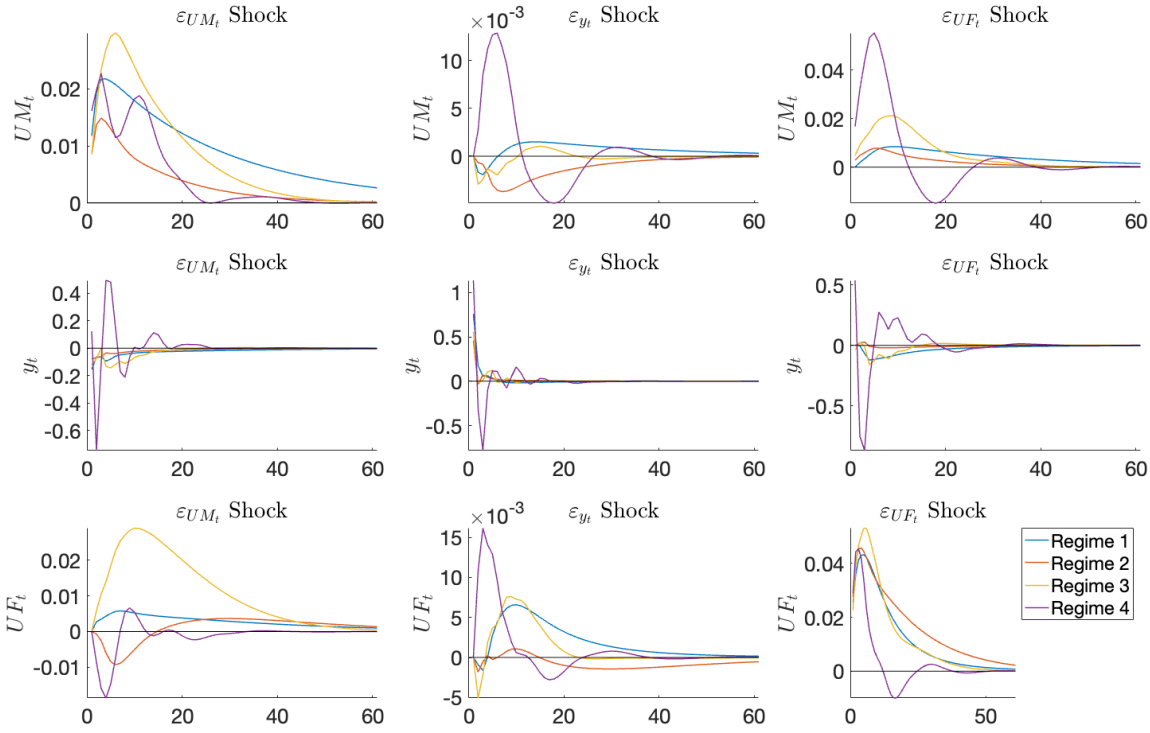

IRFs obtained from the baseline nonrecursive SVAR for $X_t := (U_{Mt}, Y_t, U_{Ft})'$, $Y_t = \Delta ip_t$ (industrial production growth), specified in Equation 24. U_{Mt} and U_{Ft} refer to the 1-month ($h = 1$) uncertainty horizon. The blue line refers to the first volatility regime (Great Inflation, 1960:M8–1984:M3); the red line refers to the second volatility regime (Great Moderation, 1984:M4–2007:M12); the yellow line refers to the third volatility regime (Great Recession + Slow Recovery, 2008:M1–2019:M11); the purple line refers to the fourth volatility regime (COVID-19 + Recovery, 2019:M12–2024:M6). Responses are measured with respect to one standard deviation changes in structural shocks.

Figure 7: IRFs in the first regime

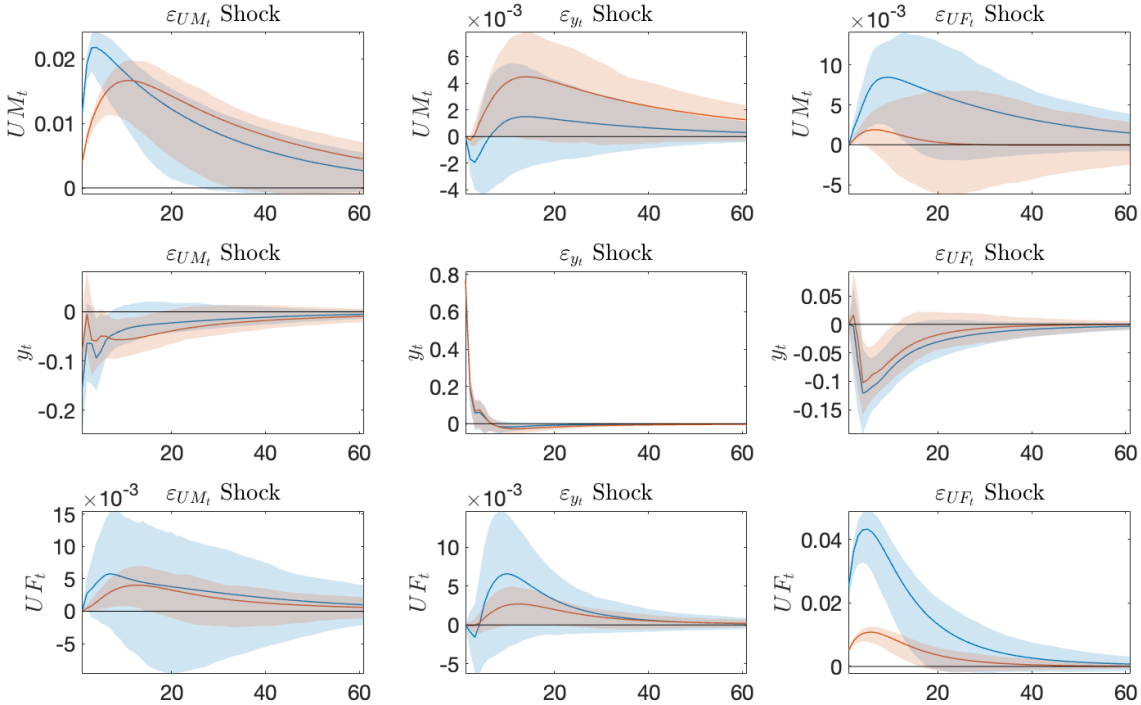

IRFs obtained in the first volatility regime (Great Inflation, 1960:M8–1984:M3) from the baseline non-recursive SVAR for $X_t := (U_{Mt}, Y_t, U_{Ft})'$, $Y_t = \Delta ip_t$ (industrial production growth), specified in Equation 24. The blue lines represent the 1-month ($h = 1$) uncertainty horizon, and blue shaded areas denote the associated 90% bootstrap confidence bands; the red lines represent the 1-year ($h = 12$) uncertainty horizon, and red shaded areas denote the associated 90% bootstrap confidence bands. Responses are measured with respect to one standard deviation changes in structural shocks.

Figure 8: IRFs in the second regime

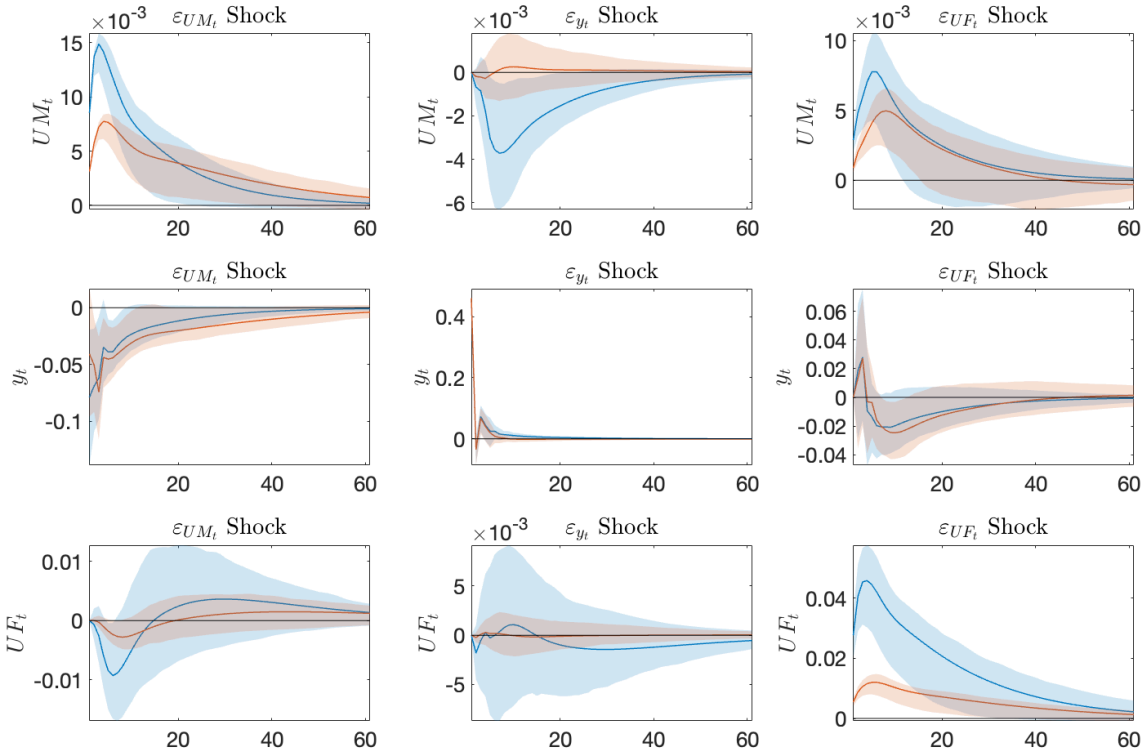

IRFs obtained in the second volatility regime (Great Moderation, 1984:M4–2007:M12) from the baseline non-recursive SVAR for $X_t := (U_{Mt}, Y_t, U_{Ft})'$, $Y_t = \Delta ip_t$ (industrial production growth), specified in Equation 24. The blue lines represent the 1-month ($h = 1$) uncertainty horizon, and blue shaded areas denote the associated 90% bootstrap confidence bands; the red lines represent the 1-year ($h = 12$) uncertainty horizon, and red shaded areas denote the associated 90% bootstrap confidence bands. Responses are measured with respect to one standard deviation changes in structural shocks.

Figure 9: IRFs in the third regime

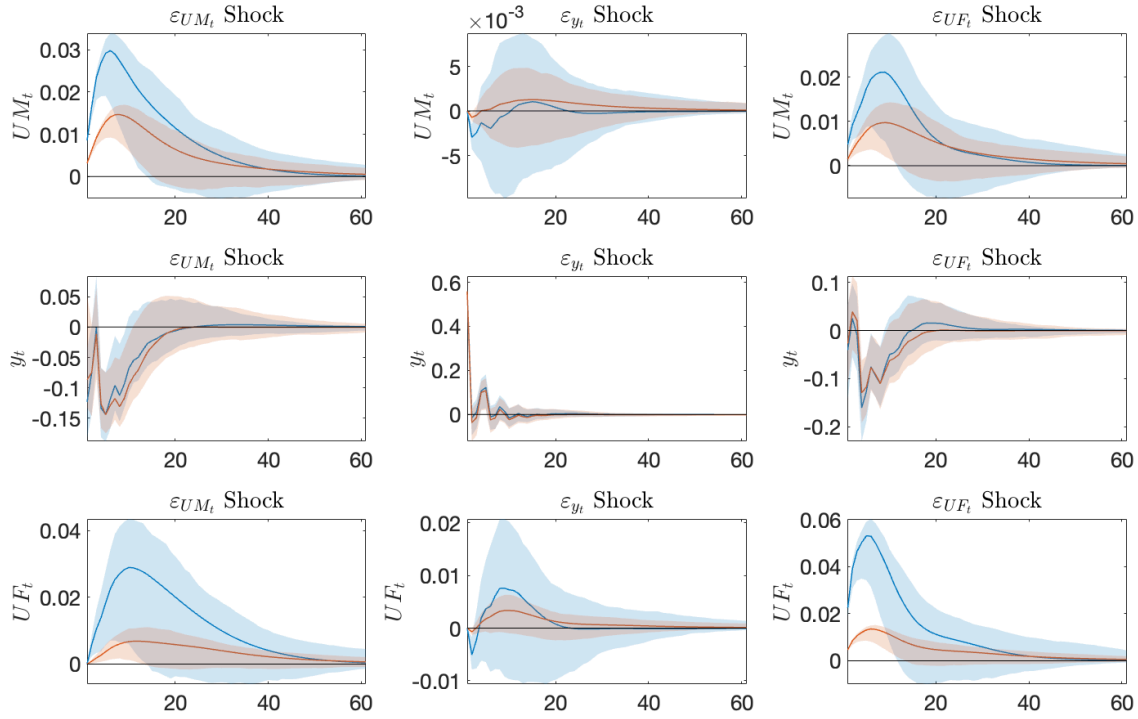

IRFs obtained in the third volatility regime (Great Recession + Slow Recovery, 2008:M1–2019:M11) from the baseline non-recursive SVAR for $X_t := (U_{Mt}, Y_t, U_{Ft})'$, $Y_t = \Delta ip_t$ (industrial production growth), specified in Equation 24. The blue lines represent the 1-month ($h = 1$) uncertainty horizon, and blue shaded areas denote the associated 90% bootstrap confidence bands; the red lines represent the 1-year ($h = 12$) uncertainty horizon, and red shaded areas denote the associated 90% bootstrap confidence bands. Responses are measured with respect to one standard deviation changes in structural shocks.

Figure 10: IRFs in the fourth regime

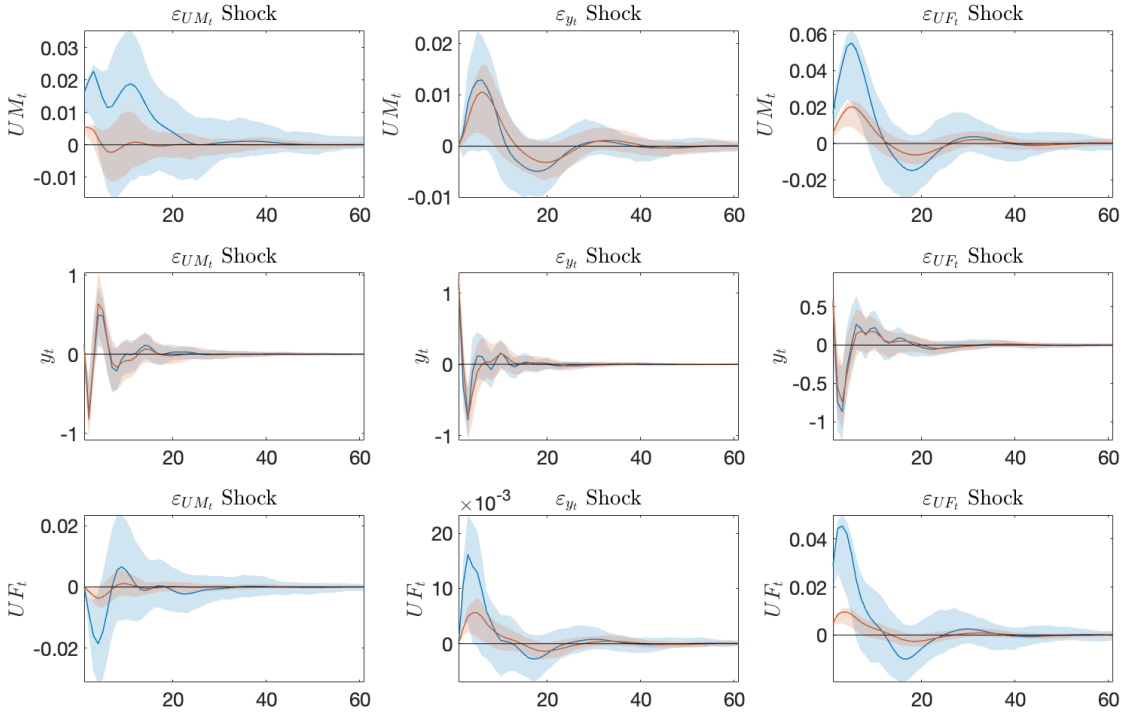

IRFs obtained in the fourth volatility regime (COVID-19 + Recovery, 2019:M12–2024:M6) from the baseline non-recursive SVAR for $X_t := (U_{Mt}, Y_t, U_{Ft})'$, $Y_t = \Delta ip_t$ (industrial production growth), specified in Equation 24. The blue lines represent the 1-month ($h = 1$) uncertainty horizon, and blue shaded areas denote the associated 90% bootstrap confidence bands; the red lines represent the 1-year ($h = 12$) uncertainty horizon, and red shaded areas denote the associated 90% bootstrap confidence bands. Responses are measured with respect to one standard deviation changes in structural shocks.

Figure 11: Forecast-Error Variance Decomposition for real economic activity

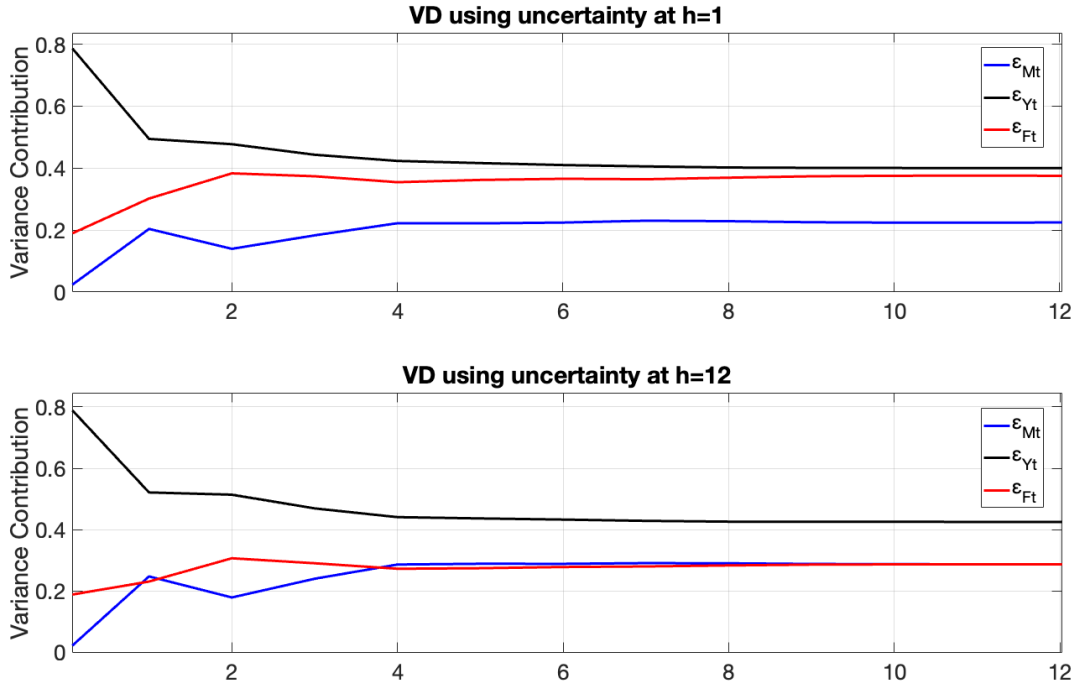

Forecast-Error Variance Decomposition for Real Economic Activity $Y_t = \Delta \text{ip}_t$ (*Industrial Production Growth*) during the COVID-19 + Recovery period, 2019:M12–2024:M6, twelve periods. The vertical axis correspond to the contribution of each structural shock in explaining the forecast-error variance of Y_t at different time spans. The first panel addresses the uncertainty at a one month horizon, while the second panel considers the twelve months horizon. The blue, black, and red lines respectively represent the variance contributions of ε_{Mt}, ε_{Yt}, and ε_{Ft}. The calculations are based on the impulse response functions derived from the specification in Equation 24.

Figure 12: IRFs across volatility regimes

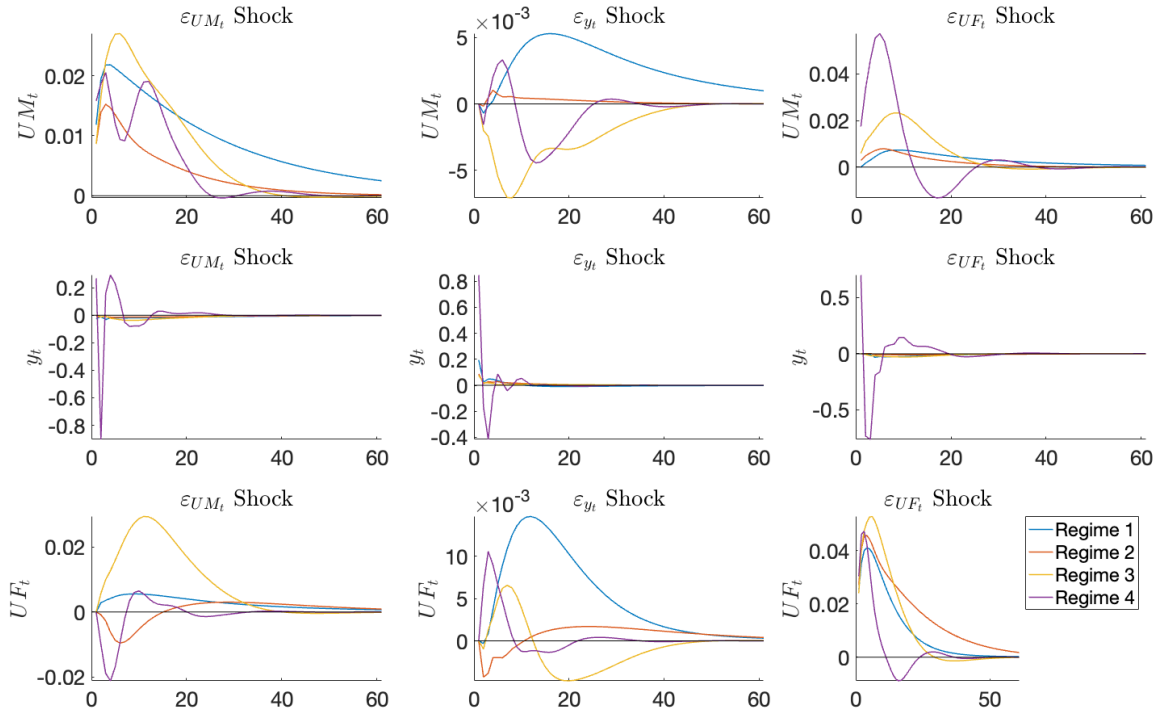

IRFs obtained from the baseline nonrecursive SVAR for $X_t := (U_{Mt}, Y_t, U_{Ft})'$, $Y_t = \Delta emp_t$ (employment growth), specified in Equation 24. U_{Mt} and U_{Ft} refer to the 1-month ($h = 1$) uncertainty horizon. The blue line refers to the first volatility regime (Great Inflation, 1960:M8–1984:M3); the red line refers to the second volatility regime (Great Moderation, 1984:M4–2007:M12); the yellow line refers to the third volatility regime (Great Recession + Slow Recovery, 2008:M1–2019:M11); the purple line refers to the fourth volatility regime (COVID-19 + Recovery, 2019:M12–2024:M6). Responses are measured with respect to one standard deviation changes in structural shocks.

Table 1: **Summary statistics for the different volatility regimes**

Period	$\hat{\Sigma}_{u_i}$	$\hat{\rho}_{u_i}$
Overall (1960:M8–2024:M6)		
log-likelihood $= 3032.3$	$\hat{\Sigma}_u = \begin{pmatrix} 1.58e-04^* & -8.89e-04^* & 1.18e-04^* \\ & 0.695^* & 0.0021^* \\ & & 7.48e-04^* \end{pmatrix}$	$\hat{\rho}_u = \begin{pmatrix} 1 & -0.0848^* & 0.342^* \\ & 1 & 0.0925^* \\ & & 1 \end{pmatrix}$
$N_{DH} = 3309.5[0.000]$		
$AR_5(u_{Mt}) = 2.373[0.7954]$		
$AR_5(u_{Yt}) = 0.119[0.999]$		
$AR_5(u_{Ft}) = 0.198[0.999]$		
GI (1960:M8–1984:M3)		
log-likelihood $= 1162.7$	$\hat{\Sigma}_{u_1} = \begin{pmatrix} 1.38e-04^* & -0.0018^* & 3.47e-05^* \\ & 0.596^* & 0.0015 \\ & & 6.44e-04^* \end{pmatrix}$	$\hat{\rho}_{u_1} = \begin{pmatrix} 1 & -0.2^* & 0.117^* \\ & 1 & 0.077 \\ & & 1 \end{pmatrix}$
$N_{DH} = 96.75[0.000]$		
$AR_5(u_{Mt}) = 2.257[0.813]$		
$AR_5(u_{Yt}) = 5.201[0.392]$		
$AR_5(u_{Ft}) = 3.422[0.635]$		
GM (1984:M4–2007:M12)		
log-likelihood $= 1392$	$\hat{\Sigma}_{u_2} = \begin{pmatrix} 7.98e-05^* & -6.14e-04^* & 7.82e-05^* \\ & 0.216^* & 4.45e-04 \\ & & 7.63e-04^* \end{pmatrix}$	$\hat{\rho}_{u_2} = \begin{pmatrix} 1 & -0.148^* & 0.317^* \\ & 1 & 0.035 \\ & & 1 \end{pmatrix}$
$N_{DH} = 356.25[0.000]$		
$AR_5(u_{Mt}) = 2.486[0.779]$		
$AR_5(u_{Yt}) = 0.244[0.999]$		
$AR_5(u_{Ft}) = 0.143[0.999]$		
GR+SR (2008:M1–2019:M11)		
log-likelihood $= 694.9$	$\hat{\Sigma}_{u_3} = \begin{pmatrix} 9.92e-05^* & -0.0013^* & 1.08e-04^* \\ & 3.29e-01^* & -9.14e-04 \\ & & 5.09e-04^* \end{pmatrix}$	$\hat{\rho}_{u_3} = \begin{pmatrix} 1 & -0.234^* & 0.48^* \\ & 1 & -0.07 \\ & & 1 \end{pmatrix}$
$N_{DH} = 103.54[0.000]$		
$AR_5(u_{Mt}) = 1.098[0.954]$		
$AR_5(u_{Yt}) = 4.051[0.542]$		
$AR_5(u_{Ft}) = 1.753[0.882]$		
C+R (2019:M12–2024:M6)		
log-likelihood $= 180.9$	$\hat{\Sigma}_{u_4} = \begin{pmatrix} 5.40e-04^* & 0.01^* & 4.83e-04^* \\ & 1.58^* & 0.016^* \\ & & 8.33e-04^* \end{pmatrix}$	$\hat{\rho}_{u_4} = \begin{pmatrix} 1 & 0.345^* & 0.72^* \\ & 1 & 0.427^* \\ & & 1 \end{pmatrix}$
$N_{DH} = 51.85[0.000]$		
$AR_5(u_{Mt}) = 1.381[0.926]$		
$AR_5(u_{Yt}) = 2.062[0.841]$		
$AR_5(u_{Ft}) = 5.963[0.31]$		
Hypothesis Tests:		
$H_0 : LR_T = 796.95[0.000]$ (no breaks in all VAR coefficients)		
$H_0' : LR_T = 419.7[0.000]$ (no breaks in VAR covariance matrix)		

Results are based on the VAR for $X_t := (U_{Mt}, Y_t, U_{Ft})'$. Top panel: estimates on the whole sample. Second, third, fourth and fifth panels: estimates on partial samples. Bottom panel: LR Chow-type tests for the null H_0 in Equation 21 and the null H_0' in Equation 22. Asterisks (*) denote statistical significance at the 10% confidence level. NDH is the Doornik–Hansen multivariate test for Gaussian disturbances. AR5 is a Breusch-Godfrey test for the absence of residual autocorrelation against the alternative of autocorrelated VAR disturbance up to 5 lags. GI, Great Inflation; GM, Great Moderation; GR+SR, Great Recession + Slow Recovery; C+R, COVID-19 + Recovery.

Table 2: **Estimated Structural Parameters with Standard Errors and Bootstrap SE**

SVAR for $X_t := (U_{Mt}, Y_t, U_{Ft})'$

$\hat{B}$	$\hat{B} + \hat{Q}_2$	$\hat{B} + \hat{Q}_2 + \hat{Q}_3$	$\hat{B} + \hat{Q}_2 + \hat{Q}_3 + \hat{Q}_4$
$\begin{pmatrix} 0.0082 & 0.0084 & 0 \\ (0.0020) & (0.0018) & \\ -0.6514 & 0.4148 & 0 \\ (0.0983) & (0.1482) & \\ 0 & 0 & 0.0254 \\ & & (0.0011) \end{pmatrix}$	$\begin{pmatrix} 0.0013 & -0.0084 & 0.0029 \\ (0.0101) & (0.0018) & (0.0006) \\ -0.4650 & 0.0031 & 0 \\ (0.0195) & (0.5613) & \\ -0.0010 & 0 & 0.0276 \\ (0.0017) & & (0.0012) \end{pmatrix}$	$\begin{pmatrix} 0.0013 & -0.0084 & 0.0048 \\ (0.0101) & (0.0018) & (0.0009) \\ -0.5678 & 0.0288 & -0.0663 \\ (0.0403) & (0.6920) & (0.0644) \\ -0.0010 & 0 & 0.0225 \\ (0.0017) & & (0.0014) \end{pmatrix}$	$\begin{pmatrix} 0.0131 & 0.0084 & 0.0172 \\ (0.0019) & (0.0018) & (0.0028) \\ -0.5678 & 0.9983 & 0.5175 \\ (0.0403) & (0.1219) & (0.1656) \\ -0.0010 & 0 & 0.0288 \\ (0.0017) & & (0.0028) \end{pmatrix}$

Model with "endogenous" macroeconomic uncertainty: 3 overidentification restrictions: LRT = 6.9976, χ^2(df=3) [0.0720]

$\begin{pmatrix} 0.0117 & 0 & 0 \\ (0.0005) & & \\ -0.1547 & 0.7566 & 0 \\ (0.0457) & (0.0320) & \\ 0 & 0 & 0.0254 \\ & & (0.0011) \end{pmatrix}$	$\begin{pmatrix} 0.0085 & 0 & 0.0029 \\ (0.0004) & & (0.0005) \\ -0.0779 & 0.4583 & 0 \\ (0.0274) & (0.0192) & \\ 0 & 0 & 0.0276 \\ & & (0.0012) \end{pmatrix}$	$\begin{pmatrix} 0.0085 & 0 & 0.0052 \\ (0.0004) & & (0.0013) \\ -0.1285 & 0.5569 & -0.0473 \\ (0.0468) & (0.0329) & (0.0503) \\ -0.0012 & 0 & 0.0225 \\ (0.0027) & & (0.0014) \end{pmatrix}$	$\begin{pmatrix} 0.0152 & 0.0025 & 0.0174 \\ (0.0022) & (0.0024) & (0.0030) \\ -0.1285 & 1.1317 & 0.5319 \\ (0.0468) & (0.1090) & (0.1623) \\ -0.0012 & 0 & 0.0288 \\ (0.0027) & & (0.0028) \end{pmatrix}$

Equation 23: Model with "endogenous" macroeconomic uncertainty in the fourth regime: 3 overidentification restrictions: LRT = 7.1757, χ^2(df=3) [0.0665]

$\begin{pmatrix} 0.0117 & 0 & 0 \\ (0.0005) & & \\ (0.0007^*) & & \\ -0.1547 & 0.7566 & 0 \\ (0.0457) & (0.0320) & \\ (0.0591^*) & (0.0408^*) & \\ 0 & 0 & 0.0254 \\ & & (0.0011) \\ & & (0.0020^*) \end{pmatrix}$	$\begin{pmatrix} 0.0086 & 0 & 0.0029 \\ (0.0003) & & (0.0005) \\ (0.0003^*) & & (0.0005^*) \\ -0.0787 & 0.4583 & 0 \\ (0.0276) & (0.0192) & \\ (\ 0.0359^*) & (0.0210^*) & \\ 0 & 0 & 0.0276 \\ & & (0.0012) \\ & & (0.0044^*) \end{pmatrix}$	$\begin{pmatrix} 0.0086 & 0 & 0.0048 \\ (0.0003) & & (0.0008) \\ (0.0003^*) & & (0.0008^*) \\ -0.1234 & 0.5569 & -0.0405 \\ (0.0439) & (0.0330) & (0.0478) \\ (0.0446^*) & (0.0611^*) & (0.0600^*) \\ 0 & 0 & 0.0226 \\ & & (0.0013) \\ & & (0.0017^*) \end{pmatrix}$	$\begin{pmatrix} 0.0162 & 0 & 0.0167 \\ (0.0016) & & (0.0027) \\ (0.0023^*) & & (0.0041^*) \\ 0.1234 & 1.1359 & 0.5367 \\ (0.0439) & (0.1084) & (0.1625) \\ (0.0446^*) & (0.1477^*) & (0.2462^*) \\ 0 & 0 & 0.0289 \\ & & (0.0028) \\ & & (0.0033^*) \end{pmatrix}$

Equation 24: Model with "exogenous" macroeconomic uncertainty: 5 overidentification restrictions: LRT = 7.4953, χ^2(df=5) [0.1863]

Likelihood ratio test between third and first (endogenous) specification: LRT = 0.4977, χ^2(df=2) [0.7797]

Likelihood ratio test between third and second (endogenous) specification: LRT = 0.3195, χ^2(df=2) [0.8523]

Estimated structural parameters based on the nonrecursive SVARs for $X_t := (U_{Mt}, Y_t, U_{Ft})'$, $Y_t = \Delta ip_t$ (industrial production growth), uncertainty at 1-month horizon, specified in Sections 3.3-3.4. "LR_T" are likelihood-ratio tests for the overidentification restrictions. Hessian-based standard errors are in parentheses; bootstrap standard errors are denoted by asterisks

Table 3: **Negative and Significant Peaks for Each Regime**

Shock to Variable	Peak Value (h=1)	Peak Value (h=12)
	First Regime	
$\varepsilon_{Yt} \to U_{Mt}$	-0.0017 (2)	NaN
$\varepsilon_{Yt} \to U_{Ft}$	NaN	NaN
$\varepsilon_{Mt} \to Y_t$	-0.1547 (1)	-0.0594 (4)
$\varepsilon_{Ft} \to Y_t$	-0.1215 (4)	-0.1026 (4)
	Second Regime	
$\varepsilon_{Yt} \to U_{Mt}$	-0.0037 (7)	NaN
$\varepsilon_{Yt} \to U_{Ft}$	NaN	NaN
$\varepsilon_{Mt} \to Y_t$	-0.0787 (1)	-0.0743 (3)
$\varepsilon_{Ft} \to Y_t$	NaN	-0.0246 (10)
	Third Regime	
$\varepsilon_{Yt} \to U_{Mt}$	-0.0030 (2)	-0.0007 (2)
$\varepsilon_{Yt} \to U_{Ft}$	-0.0051 (2)	-0.0007 (2)
$\varepsilon_{Mt} \to Y_t$	-0.1440 (5)	-0.1440 (5)
$\varepsilon_{Ft} \to Y_t$	-0.1609 (4)	-0.1293 (4)
	Fourth Regime	
$\varepsilon_{Yt} \to U_{Mt}$	NaN	NaN
$\varepsilon_{Yt} \to U_{Ft}$	NaN	NaN
$\varepsilon_{Mt} \to Y_t$	-0.7475 (2)	-0.8236 (2)
$\varepsilon_{Ft} \to Y_t$	-0.8698 (3)	-0.7439 (3)

The highest negative (significant) responses of $Y_t = \Delta$ipt (industrial production growth) to one standard deviation changes in macroeconomic (ε_{Mt}) and financial (ε_{Ft}) uncertainty shocks, and the highest negative (significant) responses of macroeconomic (U_{Mt}) and financial (U_{Ft}) uncertainties to one standard deviation change in real economic activity shocks (ε_{Yt}), at the one-month ($h = 1$) and twelve months ($h = 12$) uncertainty horizons, are obtained from the non-recursive SVAR for $X_t := (U_{Mt}, Y_t, U_{Ft})'$ specified in equation 24. In parenthesis, the number of months after the shock at which the highest negative peak is reached is indicated.